UNIVERSITY OF OKLAHOMA

GRADUATE COLLEGE

A SUB-DAILY SEVERE WEATHER CLIMATOLOGY AND ITS IMPLICATIONS

FOR FORECASTING

A THESIS

SUBMITTED TO THE GRADUATE FACULTY

in partial fulfillment of the requirements for the

Degree of

MASTER OF SCIENCE IN METEOROLOGY

By

MAKENZIE JO KROCAK
Norman, Oklahoma
2017

A SUB-DAILY SEVERE WEATHER CLIMATOLOGY AND ITS IMPLICATIONS
FOR FORECASTING

A THESIS APPROVED FOR THE
SCHOOL OF METEOROLOGY

BY

_____
Dr. Harold Brooks, Chair

_____
Dr. Cameron Homeyer

_____
Dr. Joseph Ripberger

_____
Dr. Susan Postawko

Acknowledgements

This work would not have been possible without the continuous support from numerous individuals. First and foremost, I would like to thank my adviser, Dr. Harold Brooks, for constantly challenging me to become a better scientist. His confidence in my work and abilities has had an enormous impact on my future goals and the confidence I have in myself.

I would also like to thank my committee members, Dr. Cameron Homeyer, Dr. Joe Ripberger, and Dr. Susan Postawko. The opportunities provided by each of them have shaped my experience as a graduate student at the University of Oklahoma. Additionally, I would like to recognize the incredible amount of technical, material, and personal support I have received from CIMMS, NSSL, and the SPC. Specifically, I'd like to thank Drs. Patrick Marsh and Jimmy Correia for their constant guidance amidst all of my Python questions.

Finally, I'd like to thank all of my friends and family members for their love and support throughout this entire process. Mom, Dad, Sean and Maddie, none of this would be possible without all of you instilling in me the belief that I can do whatever I set my mind to. Also, thank you to Lauren Walker, Josh Gebauer, Allie Brannan, and everyone else at Iowa State and the University of Oklahoma who have been constant sounding boards for all of my successes and failures. Lastly, thank you to Matt Flournoy for supporting every crazy thought, idea, and adventure from day one.

Table of Contents

List of Figures

Abstract

While there has been an abundance of research dedicated to the seasonal climatology of severe weather, very little has been done to study hazardous weather probabilities on smaller scales. Using a similar process to the Brooks et al. (2003a) creation of local daily climatological tornado estimates, local hourly climatological estimates of tornado and hail event probabilities were developed using storm reports from the NOAA Storm Prediction Center. These estimates begin the process of analyzing tornado and hail frequencies on a sub-24 hour scale.

Further work began to investigate characteristics of the local climatology, including how the diurnal cycle varies in space and time. Hourly tornado probabilities are peaked for both the annual and diurnal cycles in the Northern and Southern Plains. However, this pattern breaks down quickly in the southeast United States (US), where there is a more variable pattern in tornado probabilities. These differences in the annual and diurnal cycle create forecasting and community response challenges unique to each region. These challenges are briefly discussed along with the associated climatological risks.

The same process was repeated using hail reports, yielding similar results to the tornado climatology. While the annual and diurnal cycles were once again more variable in the southeast US than in the Plains, the differences in the cycles were not as pronounced as in the tornado climatology.

This work is part of a larger effort to provide background information for probabilistic forecasts of hazardous weather that are meaningful over broad time and space scales, with a focus on scales broader than the typical time and space scales of the

events of interest (including current products on the "watch" scale). A large challenge

remains to continue describing probabilities as the time and space scales of the forecast

become comparable to the scale of the event.

Chapter 1: Introduction and Background

1.1 Motivation

Severe weather, specifically tornadoes and hail, cause large amounts of damage to life and property every year (National Oceanic and Atmospheric Administration (NOAA) Storm Prediction Center). Hail damage, in particular, produces economic impacts to nearly every region of the United States (US). Even those areas that do not see many hail events, like the Southeastern US (SE US), still experience large economic loss due to crop damage to fruit and other sensitive species (Chagnon 1972). Tornadoes also produce both economic and life threatening impacts, as shown in Ashley (2007). This work showed through an analysis of tornadic fatalities in the US that most fatalities occur in the southeast portion of the country, where there is a higher proportion of elderly residents and mobile homes. The juxtaposition of multiple types of severe events and certain demographics makes the SE US particularly vulnerable. Carbin et al. (2013) examined the current challenges facing tornado forecasters and discussed the specific need for a forecasting paradigm shift to continue to increase lead times for these types of events. One way to change the current hazardous weather forecasting paradigm is to include a probability of occurrence in forecast products. Vescio and Thompson (2000) looked at the accuracy of probability of tornado occurrence values in weather watch products. They concluded that adding probabilistic information was useful in highlighting the area of greatest threat within the watch.

To this end, a recent NOAA initiative, called the Forecasting a Continuum of Environmental Threats (FACETs) project, aims to usher in a new forecasting paradigm that includes probabilistic information. The project is working to transform the current

dichotomous severe weather watch and warning system into one with a continuous stream of probabilistic hazardous weather information (Rothfusz et al. 2014). Regarding the larger end of the temporal and spatial scales of these forecasts (24 hours), we looked at the distribution of all severe reports from the Storm Prediction Center's (SPC) event archive and found that more than 95% of reports within a 24 hour convective outlook day (12 UTC to 12 UTC) are contained in a 4 hour period. Therefore, the 24 hour convective outlook probabilities can be interpreted as 4-hour convective probabilities. This information is vital in understanding how forecasters can create and maintain a continuous stream of severe weather information on shorter (8-2 hours) time scales, as the FACETs project is aiming to implement. Workload could be greatly reduced if forecasters generally need to be concerned with a 4-hour period of the day rather than all 24 hours.

The current severe weather forecasting system consists of a 24-hour convective outlook, followed by a "watch" (which usually lasts on the order of 2-8 hours), followed by a warning (which usually lasts less than 1 hour). Therefore, it's logical that climatological severe weather information is calculated on the order of days at the finest scales (to help forecasters with their outlook creation). However, if forecasters are going to be expected to create severe weather probabilities on sub-daily scales, there needs to be climatological background information that can support these types of forecasts. Additionally, general improvement of severe weather forecasts may come from understanding how their climatological frequency is distributed throughout the year as well as throughout the day. Thus, current climatological information on monthly, weekly, or daily (at best) scales is too coarse to be of aid with future hourly and sub-

hourly forecasts of these events. Conversely, sub-daily climatological values can also provide event context for emergency managers and community members once these forecasts are disseminated. Without baseline climatological information, how is an end user supposed to know if today's threat is "high" or "low"? Should users start to worry about severe weather when the probabilities are at 0.01%? 2%? 30%? For these reasons, the need to have climatological probabilistic information of severe weather events on a sub-daily scale has become evident. To that end, an hourly climatology of tornadoes and severe hail events was developed using similar methods to the work described in Brooks et al. (2003a). In addition to the hourly climatological estimates, an analysis of the spatial and temporal differences between hourly estimates was also executed, and impacts of those differences are discussed.

1.2 Previous Tornado Climatologies

There have been numerous attempts to quantify the climatological risk of severe hazards. Many of the tornado climatological estimates are created using only parts of the total report database in an attempt to reduce the errors associated with it. Those studies that use only (E)F2 and greater reports (Brooks and Doswell 2000, Coleman and Dixon 2014, Concannon et al. 2000) have found the maximum probability of tornado occurrence to be in an L-shaped pattern extending from Iowa down into Oklahoma and then east into Mississippi and Alabama (See Figure 1 from Brooks and Doswell 2000). Some of the highest risk areas are often located in the southeastern portions of the US (SE US): the threat tends to start in these areas in the beginning of the year and then move north in the summer before returning in the fall and winter. Another method

discussed in Kelly et al. (1978) attempted to remove report bias from the record, while

still retaining 80% of the reports. They converted report times to mean solar time and

then analyzed patterns in the remaining reports. Results showed that most violent
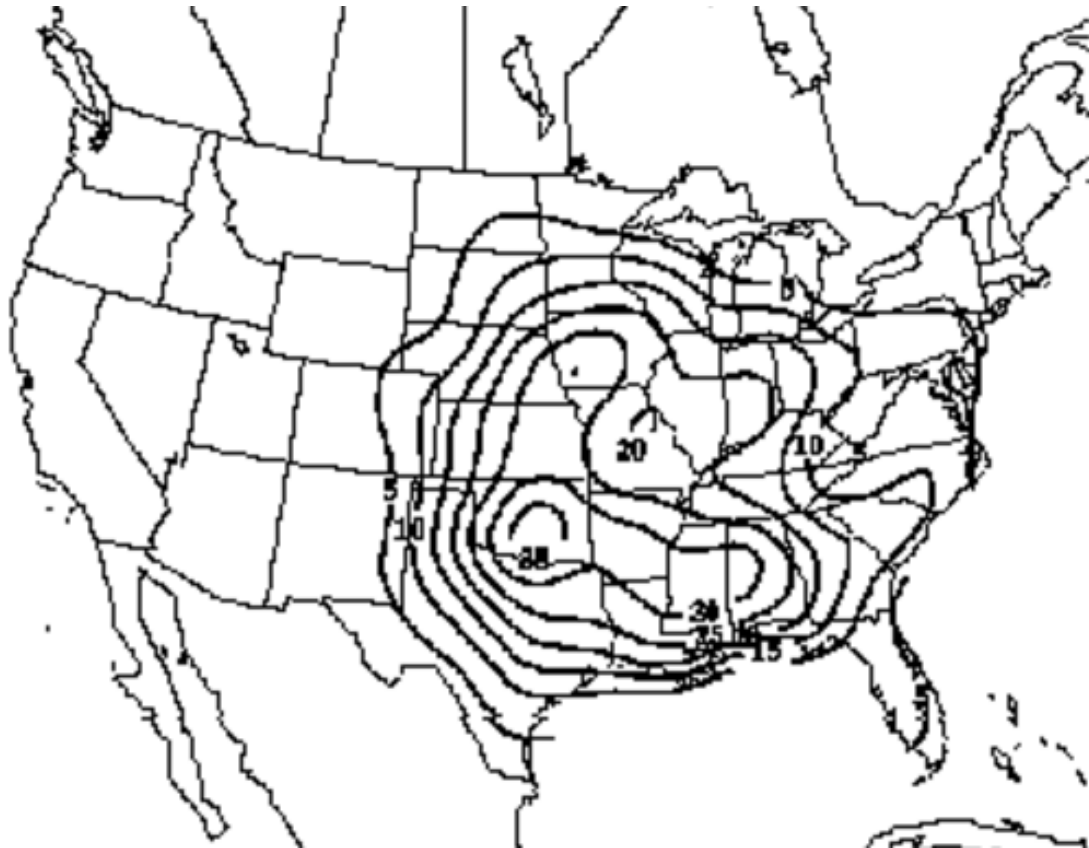
Figure 1.1: Mean number of days per century with at least one F2 or greater tornado touching down in an 80km grid box. Contour interval is 5 days with lowest contour 5 (Brooks and Doswell 2000, Figure 1).

tornadoes occur on outbreak days, except in the SE US. Throughout the literature, one

common theme was the differences in climatological tornado patterns between the

Plains and the SE US. The latter often sees a high number of nocturnal tornadoes, which

is analyzed on a climatological scale in Kis and Straka (2009). Environmental data

taken from model proximity soundings around nocturnal tornadoes revealed that

environments commonly found in the fall and winter months in the SE US (with low instability but substantial low-level vertical wind shear) which were previously thought to not be supportive of these storms often produced them. Rasmussen and Blanchard (1998) also looked at environmental factors supportive of tornado reports, but this work focused on supercell characteristics. Shear and Convective Available Potential Energy (CAPE) values were found to weakly discriminate between tornadic and non-tornadic environments, particularly in the Plains. Finally, Schaefer et al. (1986) found that probabilities for any tornado occurrence for all tornadoes with an F4 rating or less were very widespread across all locations east of the Rocky Mountains, including the Plains, the Ohio River valley and the SE US.

1.3 Climatological Tornado Patterns

Changes to the climatology of tornado occurrence throughout the latter half of the 20th century have been investigated a number of times. Verbout et al. (2006) found there to be an average of 18 "big tornado days" per year (defined as greater than 8 EF1 or higher tornadoes per day). However, multiple studies including Brooks et al. (2014) and Elsner et al. (2014) found a decrease in the number of days per year with at least one tornado report. Essentially, each day has a lower probability of a tornado occurring, but if tornadoes do occur, then there is a higher probability of having multiple tornadoes. Therefore, the number of days with tornadoes has decreased over the last six decades, but the number of "big tornado days" (or outbreak days) has increased. In addition to these findings, there are indications that intraseasonal tornado climatology characteristics are also changing. Tippet (2014) used a tornado environment index to

assess whether these changes are due to deviations in reporting practice or actual atmospheric changes. Results showed that changes did occur to this index after 2000, indicating that there is more volatility to US tornado frequencies, meaning one year may have very few reports, and the next could be a record high report year. Finally, Long and Stoy (2014) and Lu et al. (2015) both found that the peak in tornado season is becoming earlier in the year, which can have huge implications for community resilience to these types of disasters.

1.4 Previous Hail Climatologies

A climatology of non-tornadic storms was produced by Doswell et al. (2005). They used hail and wind reports of the SPC database, gridded and smoothed the reports in a similar way to Brooks et al. (2003a) and found a preference for severe reports in the Plains. The cycle to this climatology followed that of the tornado climatology, which starts in the southern states and moves north throughout the summer before returning to the SE US during the fall and winter. Additionally, a severe hail climatology was developed by Cintineo et al. (2012) and found a broad max of hail occurrence in the Plains and a secondary axis in the SE US. The early spring months (March-May) saw the most reports in the SE US, but the most active month was June in the Plains.

Allen and Tippett (2015) describe one of the more holistic climatological hail estimate studies in which they use all reports greater than 0.75 inches. While they acknowledge the issues with hail reporting practices (like the higher density of reports surrounding road networks and the sharp increase in reports with the development of communication technologies), they also argue that these estimates are still robust when

6

researchers consider overall patterns and statistics. The methods used to create this climatology closely resemble the gridding and smoothing procedures used in Brooks et al. (2003a), where researchers project reports onto an 80 km grid and use Gaussian kernels to smooth those report values. One of the major caveats to this work is the reduction of time period to the last 10-20 years due to the linear increase in hail days (days with at least one hail report) outside of this time period.

Chapter 2: Data and Methods

2.1 Storm Reports

The storm reports used to build the hourly hail and tornado climatology come from the Storm Prediction Center's (SPC) Severe Report Database (Schaefer and Edwards 1999). Reports are collected from National Weather Service offices, quality controlled to remove erroneous and duplicate reports, and then sent to the SPC where the times are then converted to Central Standard Time. The tornado climatology uses reports from 1955 to 2015, while the hail climatology uses reports from 1963 to 2015. There are a number of changes that occurred in reporting practices during the earlier years of the severe weather report database (Doswell and Burgess 1988) These years were chosen to minimize the impact of these changes.

There are a number of studies that have attempted to analyze the errors and inconsistencies with severe weather reports in the United States (e.g. Doswell and Burgess 1988, Anderson et al. 2007, Brooks and Doswell 2009b). First, reports are subject changes in reporting practices. For example, the change in the definition of severe hail from 0.75 inches to 1.00 inches in 2010 had an impact on the number and process of reporting severe hail events. Additionally, road networks and population may also have an impact on reporting practices. Hail is particularly vulnerable to road placement, as those events are generally reported after it occurred (when people see it on the ground), whereas tornadoes are often seen from miles away, making those events less vulnerable to where the reporter is located (Allen and Tippett 2015). Next, some events that occur where there is a low population density may not be reported, whereas many more reports occur in locations with a high population density (Anderson et al.

2007, Gall et al. 2009, Brooks and Doswell 2009b). Finally, tornado ratings are often underestimated due to the Fujita and the later implemented Enhanced Fujita scale system. Since it is a damage scale, damage indicators are necessary for an accurate assessment of tornado intensity. If a tornado occurs in a rural area and does not hit many structures, the tornado will likely be underrated (Doswell and Burgess 1988). Anderson et al. (2007) found that many tornadoes in the Southern Plains are likely underrated for exactly this reason.
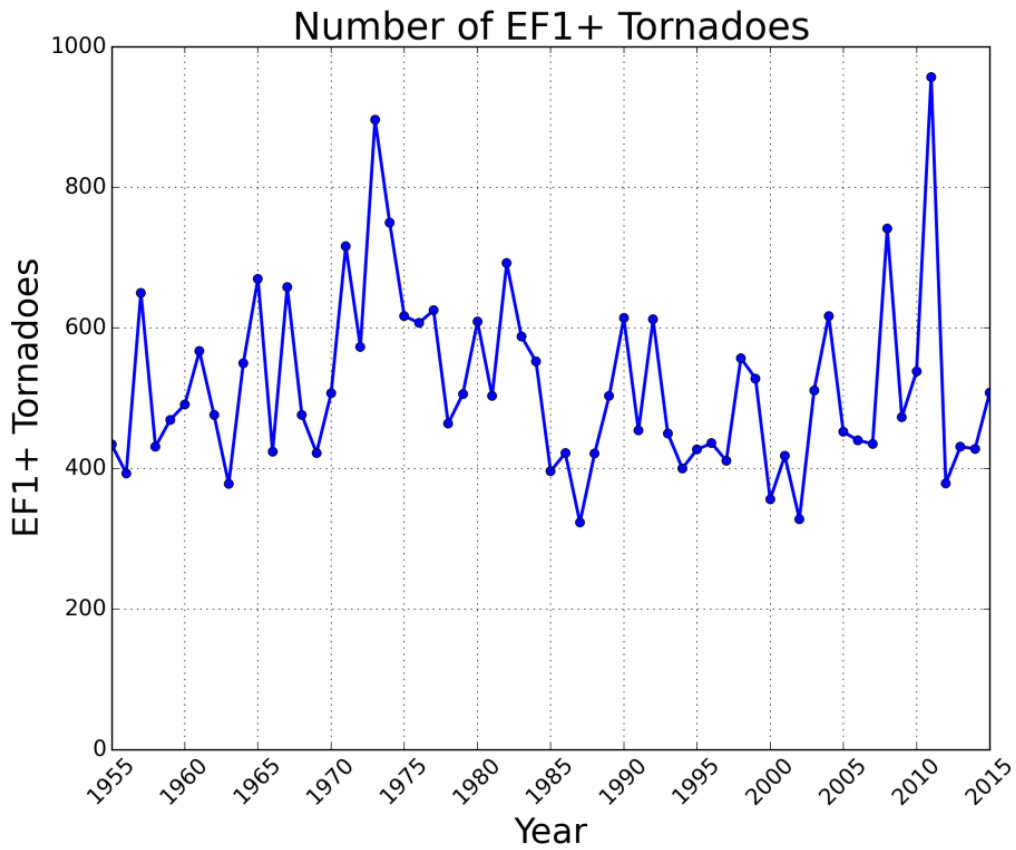
Figure 2.1: Number of EF1+ tornado reports by year.

This work uses all EF1+ tornado reports (on the Enhanced Fujita scale, Doswell et al. 2009) between the years 1955 and 2015. Brooks et al. (2003a) showed that while

the number of tornado reports nearly doubled between the mid-1950s and the early 2000s, the number of tornado days (days where at least one tornado was reported somewhere in the US) only rose 10-15%. Other work has also shown that the number of strong and violent tornadoes remained relatively constant throughout the period (Schaefer and Schneider 2002). Additionally, we show that when the dataset is restricted to only EF1+ tornadoes, there is no significant trend in the number of reports (Figure 2.1). Given this lack of increase in reports, we are confident that our calculated climatological estimates are robust.

Next, the hail climatology uses all reports greater than 1.25 inches. While Allen
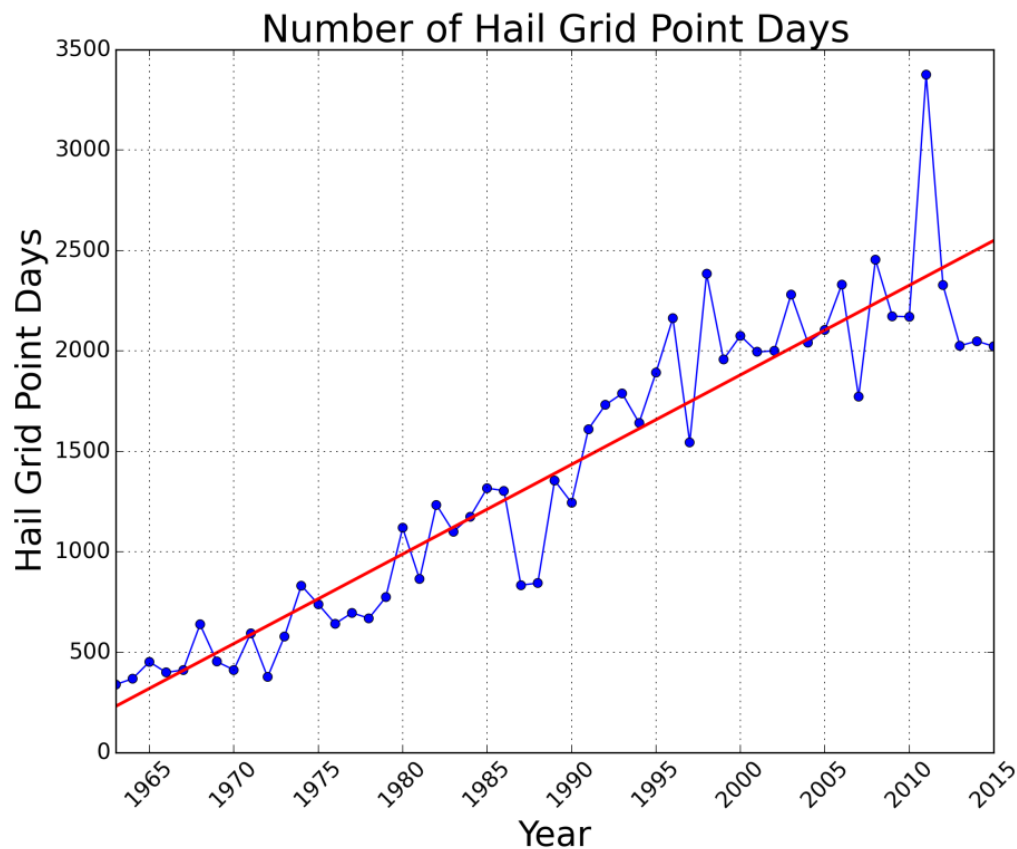
Figure 2.2: Number of hail grid point days by year. The linear regression is plotted in red.

and Tippett (2015) found no significant trend in the number of hail days per year at any size threshold, they did find a positive, linear trend in the number of hail grid point days (number of grid points with at least one report in a day) per year, although the results were not statistically significant. Since this work is using hail reports all the way back to 1963, and since there is a positive, linear trend in the hail grid point days throughout that time period (Figure 2.2), detrending methods (described in section 2.5) were used to create the final hourly hail climatology following the methods outlined in Allen and Tippett (2015) to ensure later years did not have more of an impact on the climatological estimates than early years.

2.2 Gridding of Reports

This study uses report gridding and smoothing processes similar to other climatology work (e.g. Thom 1963, Brooks et al. 2003a). Reports were assigned a grid point based on the location of the report (touchdown location for tornadoes) and the hour of the year (where the first hour is hour 1 and the last hour is hour 8784) the report occurred. Locations were plotted on a Lambert conformal grid with an 80 kilometer horizontal grid spacing. The grid is true at 39.8° N. These characteristics were chosen because they are similar to those currently used by forecasters in the SPC. The temporal location of the report was calculated based on number of hours after 12 UTC on January 1st. The full grid contained 8784 hours, equal to 366 days. If the year being analyzed was not a leap year, all reports after February 28th were transposed onto a 366 day year (i.e. 24 hours was added onto the hour calculation). Grid boxes that contained a report were assigned the number 1, with all other grid boxes assigned a 0. Therefore, after

smoothing the 1s and 0s, these values represent the probability of a tornado or hail

report occurring within the 6400 square kilometer grid box within that hour.

2.3 Spatial Smoothing of Grids

To create reasonable probabilities over long time periods, the hourly gridded

reports were smoothed both temporally and spatially using nonparametric density

estimation (Silverman 1986). First, grids were smoothed spatially at each hour using a

two-dimensional Gaussian kernel, where P is the smoothed probability, N is the total

number of grid boxes with events, d is the distance from the point location to the report

location, and σ is the standard deviation of the Gaussian distribution, or the smoothing

parameter:

$$P = \sum_{n=1}^{N} \frac{1}{2\pi\sigma^2} e^{-\frac{d^2}{2\sigma^2}}$$

The standard deviation used for the spatial smoothing was 120 km. Although Dixon et

al. (2013) found that the ideal spatial smoothing radii was around 150 km, they

acknowledged that each season has its own ideal radii, and that 150 km simply

represents the best combination of all of them. However, Brooks et al. (2003a) found

that 120 km (or 1.5 grid spaces) yielded the most realistic climatological values without

over-smoothing smaller scale patterns. For these reasons, we chose to use 120 km to

smooth our values spatially.

2.3 Temporal Smoothing of Grids

Since this work focuses on the sub-daily estimates of severe weather events, the

temporal smoothing procedures become critical for accuracy of our final estimates.

First, we smoothed all values at the same time of the day using a one-dimensional

Gaussian kernel with a 15 day standard deviation, as shown below:

$$P = \sum_{n=1}^{N} \frac{1}{2\pi\sigma^2} e^{-\frac{t^2}{2\sigma^2}}$$
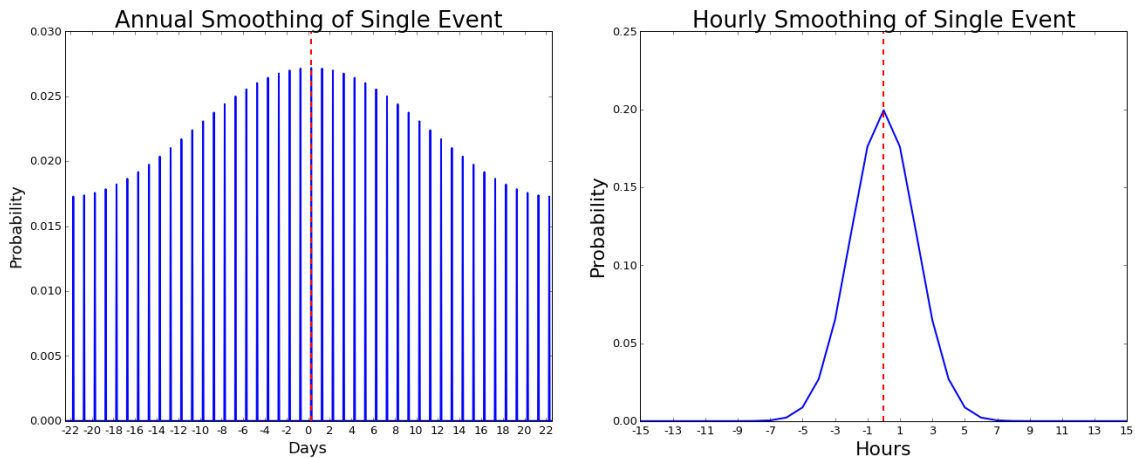
Figure 2.3: Results of smoothing a single event using a Gaussian kernel over the annual cycle (left) and the daily cycle (right).

For example, all 00 UTC hour values (every 24th value starting with the first 00 UTC

hour) were gathered and then smoothed with the 15 day kernel shown above, where t is

the distance from the hour value being smoothed. The resulting field is shown in Figure

2.3 (left), where every 24th hour contains a smoothed value.

Next, values were smoothed within the same day using a 2 hour kernel. The

right plot in Figure 2.3 shows the result of this smoothing, which shows a sharper

decrease in smoothed values as compared to the annual smoothing.

The reason for this multi-step smoothing process was to ensure the creation of a

seasonal tornado cycle, while also preserving the smaller scale diurnal cycle. Again, it

was critically important to preserve the daily cycle of these events so that forecasters

13
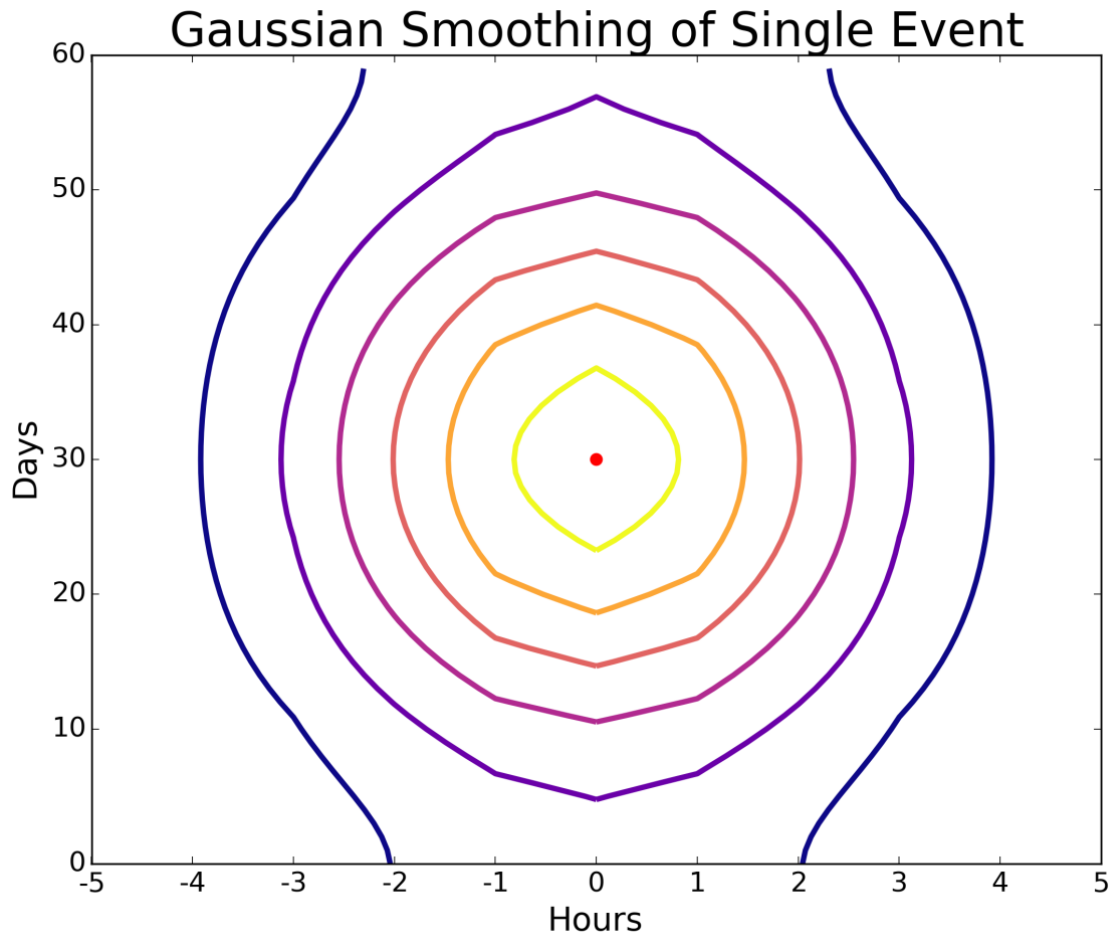
Figure 2.4: Temporal Gaussian smoothing technique described above for a single event, denoted by the red dot.

will have accurate and reliable background information when making sub-daily probabilistic forecasts of severe events under the FACETs paradigm. Figure 2.4 shows how a single event would be smoothed using this technique. While a single event had a relatively large impact on corresponding values 40-50 days out, that same event only had marginal impacts on adjacent values 4-5 hours out.

2.4 Creation of a Sixty-One Year Tornado Climatology

The aforementioned gridding and smoothing technique was executed for reports in a single year for each year from 1955 to 2015.This time period was because there is a sharp increase in the number of tornado reports between 1954 and 1955, indicating a lack of reliability for the reports prior to 1955. After all 61 grids of size 45 by 66 by 8784 were created, the mean probability for each grid box was calculated, resulting in a single grid with the same dimensions as each yearly climatology grid. This allowed for an overall hourly climatology to be analyzed, as well as climatological changes throughout the 61 year period.

2.5 Creation of a Fifty-Three Year Hail Climatology

The hail reports used were between 1963 and 2015. The beginning portion of the reports were not used because there was once again a sharp increase in reports between 1962 and 1963, indicating that the earlier reports were unreliably gathered. While the gridding and smoothing of the hail reports are the same as that for the tornado reports, the creation of the climatology differs. Due to the linearly increasing number of hail grid point days per year, smoothed probabilities were weighted based on the number of hail grid point days per year relative to all other years. This was done by calculating a linear regression (plotted in Figure 2.2) and then calculating a weight for each year equal to:

$$w = \frac{g_{2015}}{g_{year}}$$

where g_{2015} is the predicted number of hail grid point days in 2015, equal to 2549.69,

and g_{year} is the predicted number of hail grid point days at the year of interest. Since

2015 has the highest number of hail grid point days, all weighted values will be greater

than or equal to one. This weighting method normalizes climatological values to 2015

values, despite the changes in number of grid point days per year. The final result is an

hourly climatology for the US on an 80 km grid.

Chapter 3: Characteristics of Hourly Tornado Probabilities

3.1 Annual and Diurnal Cycles

After the gridding and smoothing process of all EF1 and higher rated tornadoes, the total climatological number of tornado touchdowns per year was calculated for any point in the US by simply adding all 8784 hourly probability values together. This result is shown below in Figure 3.1. Values in central Oklahoma and north Texas are very similar to values in Mississippi and Alabama. By this measure, one might deduce that the tornado threat in these areas is the same, however, the distribution of this total threat is location-specific. In fact, the hourly climatology highlights some
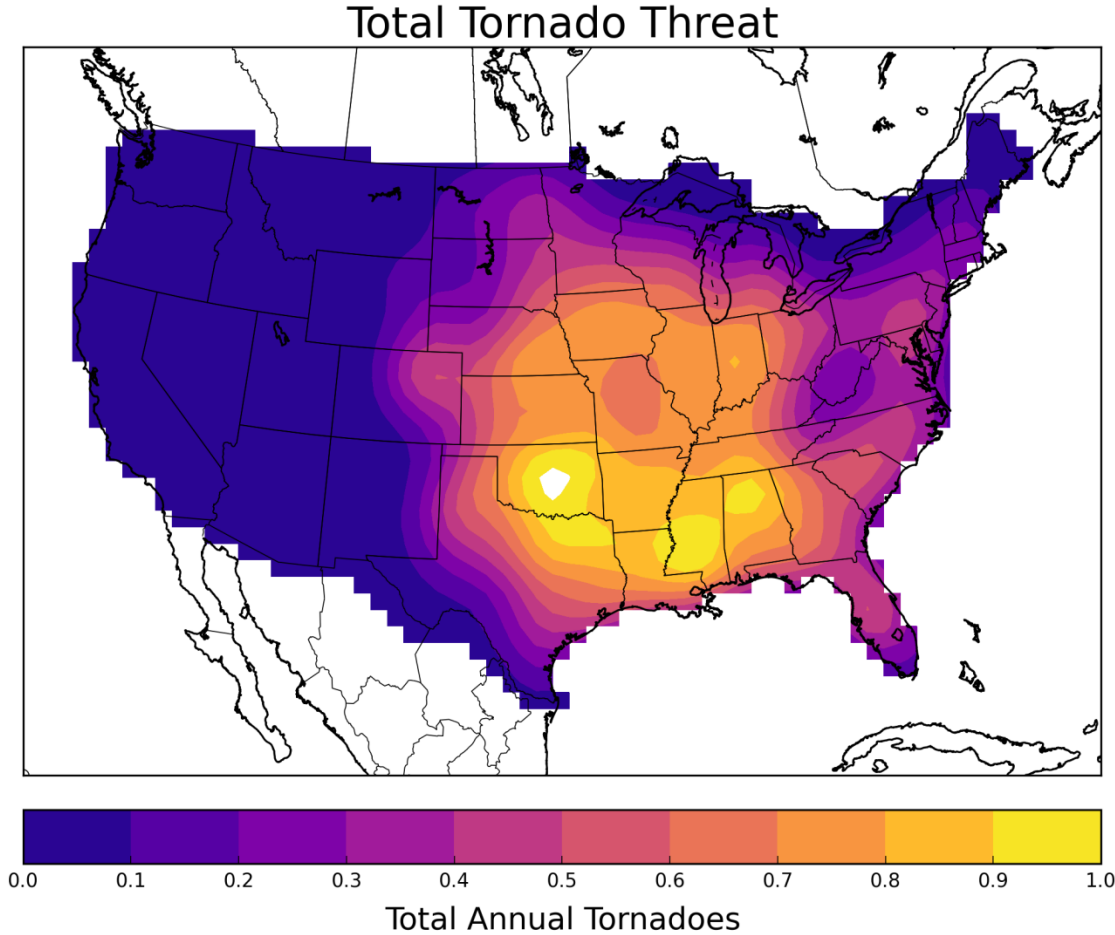
Figure 3.1: The total number of tornadoes for every grid point across the United States.

very important differences in how the tornado threat is distributed. These differences and the impacts they have on disaster response are discussed throughout this chapter.

The main purpose of the multi-step smoothing process described in Chapter 2 was to maintain the diurnal cycle of tornado probabilities while also showcasing the annual cycle. This resulted in adjacent values of total daily tornadoes that look very similar, with adjacent hourly probabilities of tornadoes that look very different. In fact, 12 hours of separation can lead to tornado probabilities that are orders of magnitude different. Following the Brooks et al. (2003a) methods, the total daily number of tornadoes is calculated by adding together all of the hourly probabilities in a 24 hour period starting at 12 UTC. Figure 3.2 shows total daily tornadoes for May 15th and May 16th. The plotted values are nearly identical, except for the portion in southeast Missouri.
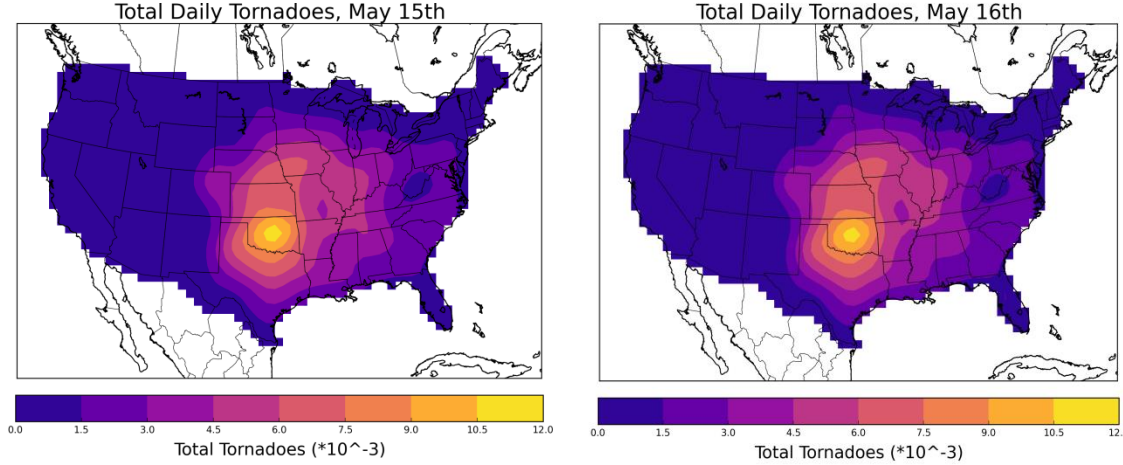
Figure 3.2: Total Daily Tornadoes for May 15th (left) and May 16th (right).

In contrast to the daily tornado values, the hourly tornado probabilities differ dramatically, which illustrates the importance of the diurnal cycle in tornado occurrence. Figure 3.3 shows the tornado probability for 10 UTC on May 15th on the

left and 22 UTC on May 15th on the right. Noting that the color bars are different by an order of magnitude, there are two peaks in the morning and only one much higher magnitude peak in the afternoon. The single peak in the Southern Great Plains in the afternoon gives us the first indication that tornado probabilities in this area are much more diurnally driven than in the SE US. Brooks et al. (2003a) also showed that the *annual* cycle of tornado probabilities is very seasonally driven in the Plains and much more variable in the SE US. This higher resolution climatology begins to show that the diurnal cycle follows much of the same pattern, with clearly peaked daily cycles in the Plains and variable cycles in the Southeast.
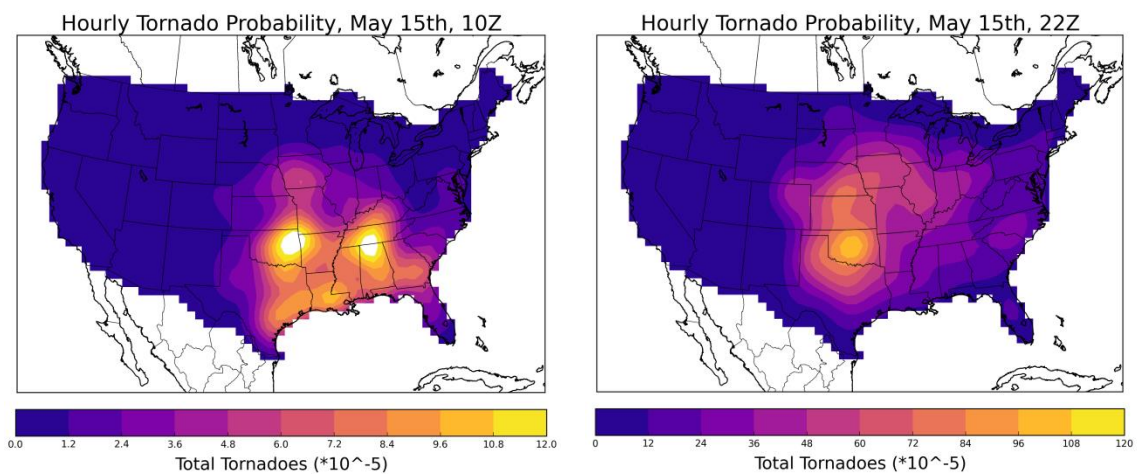
Figure 3.3: Hourly tornado probability at 10 UTC on May 15th (left) and 22 UTC on May 15th (right). Note scale of the maps differs by an order of magnitude.

3.2 Spatial and Temporal Differences in Tornado Probabilities

While many studies have shown the spatial differences in tornado threats throughout the year (e.g. Kelly et al. 1978, Concannon et al. 2000, Brooks and Doswell 2000, Brooks et al. 2003a, Ashley 2007 etc.), very few have shown the differences in how the tornado threat changes throughout the day. This hourly tornado climatology

gives us the ability to identify patterns and differences in the diurnal cycle across the country.
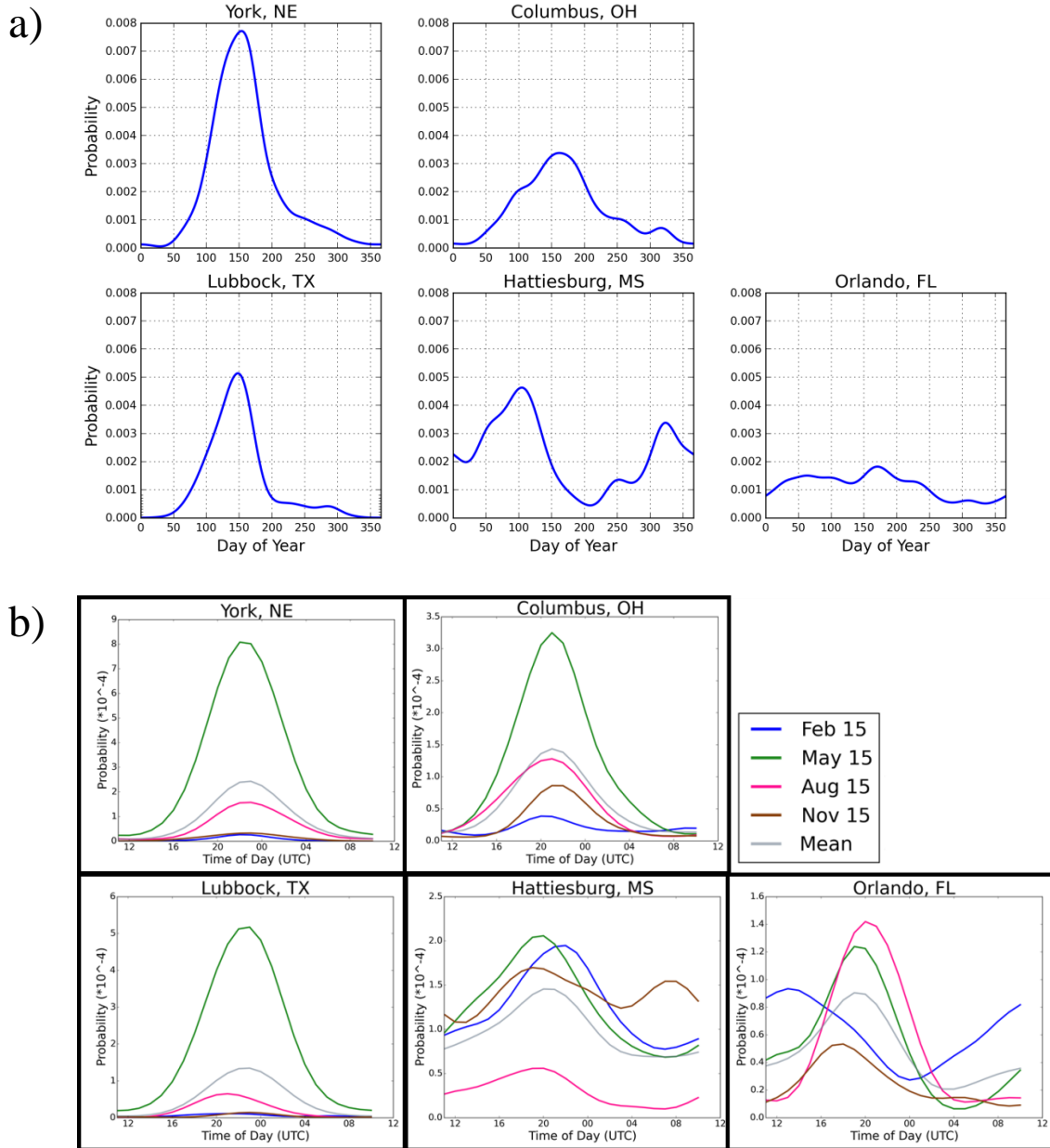
Figure 3.4: a) Annual cycles of daily tornado probability. b) Daily cycles of tornado probability. Note the y-axis scales are different for each location.

The annual cycles of tornado probability are plotted for York, NE; Columbus, OH; Lubbock, TX; Hattiesburg, MS; and Orlando, FL in Figure 3.4a. The daily tornado

probability cycles for those same locations are plotted in Figure 3.4b. The different colors in Figure 3.4b represent different times of the year (the 15th of February, May, August, and November) with grey being the mean of the four other cycles. One of the most obvious differences between the five sites is the distinction between the Plains locations and the SE US locations. As seen in the annual cycles (Figure 3.4a) York, Columbus and Lubbock all show a strong seasonal cycle with May-June having the strongest peak (around 0.0008, 0.0003 and 0.0005 respectively for the May 15th values in Figure 3.4a). Hattiesburg and Orlando do not show the same strong seasonal cycle. The different times of the year have very similar magnitudes of peak probability, with the exceptions of August in Hattiesburg and November in Orlando.

In addition to a weak seasonal cycle for the SE US locations, there is also a weak daily cycle for these locations (Figure 3.4b). While York, Columbus, and Lubbock all show a strong peak around 20-00Z during the warm season with very low probabilities outside of the peak, Hattiesburg and Orlando do not have the same pattern. Probabilities outside of the peak remain relatively high, indicating the diurnal cycle does not play as strong of a role in tornado frequency in the SE US as compared to the Plains. These results reinforce those seen in Section 3.1, where Plains locations have a very strong peak in the afternoon that is not matched in magnitude in the SE US.

To visualize the peak tornado time and magnitude for multiple locations, the values in Figure 3.4b for the 15th of February were plotted on a map of the US in Figure 3.5. The size of the square marker is directly proportional to the total number of tornadoes (the area under the blue curves in figure 3.4) and the color of the marker represents the hour with the highest probability. The stars indicate the locations of the

21
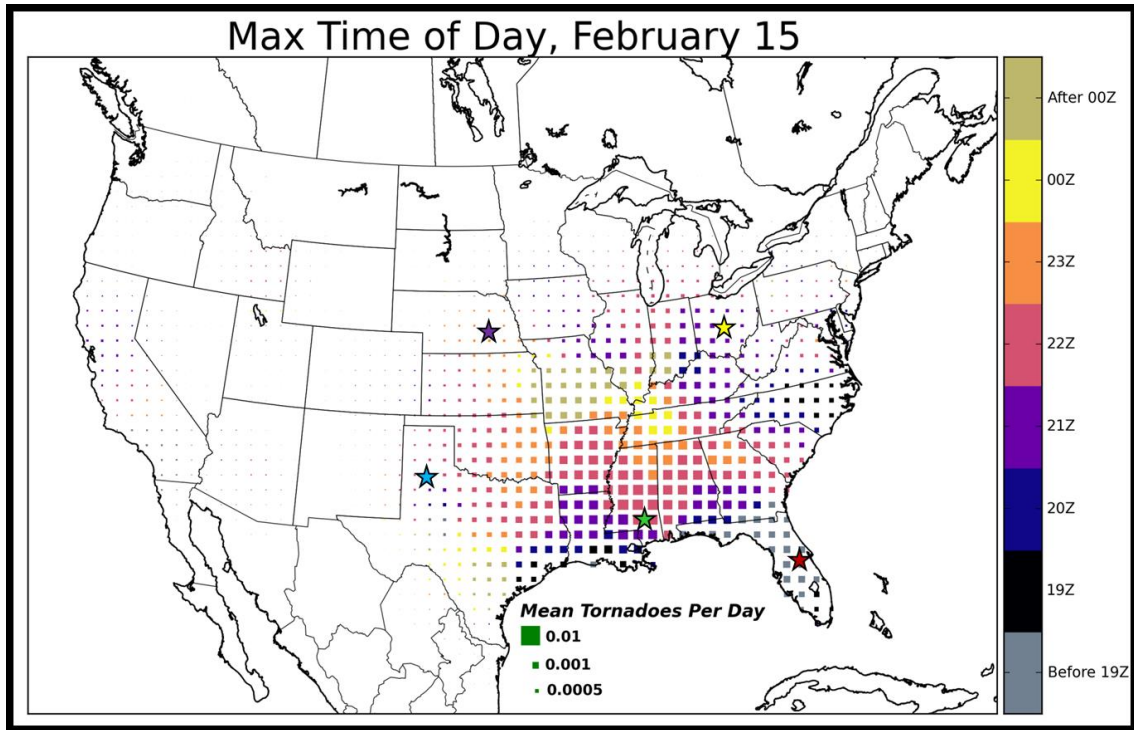
Figure 3.5 Mean tornadoes per day (represented by the size of the square) and peak time (represented by the color of the square) for the 15th of February.

curves plotted in Figure 3.4. The color bar is truncated from 19-00Z, with earlier hours in grey and later hours in beige. Nearly all of the early hours (grey in color) were in the Florida peninsula during the winter months, indicating that mesoscale influences (e.g. land/sea breezes) dominate tornado occurrence during these times and locations.

The most noticeable pattern is in the location of the peak times. The early peak hours (black, blue and purple colors) are in the south and southeast portion of the visible markers, with peak times becoming progressively later to the north and west, such that the pink, orange, and yellow colors are concentrated in the northwest portion of the visible markers.

To visualize these patterns throughout the year, an animation of the 15th day of each month was created. The maps for February, May, August, and November are

plotted in Figure 3.6. There are a number of interesting patterns that emerge when both

spatial and temporal patterns can be explored simultaneously. First, the 23Z-00Z peak

(orange and yellow in color) is situated in the SE US during the cool season, and then

moves west into the Southern Great Plains during April and May. It then expands and

moves due north during the summer months before retreating back to the SE US. This

peak time mirrors the location of the peak intensity in the Plains, indicating that most

Plains tornadoes occur in the late afternoon and early evening hours.
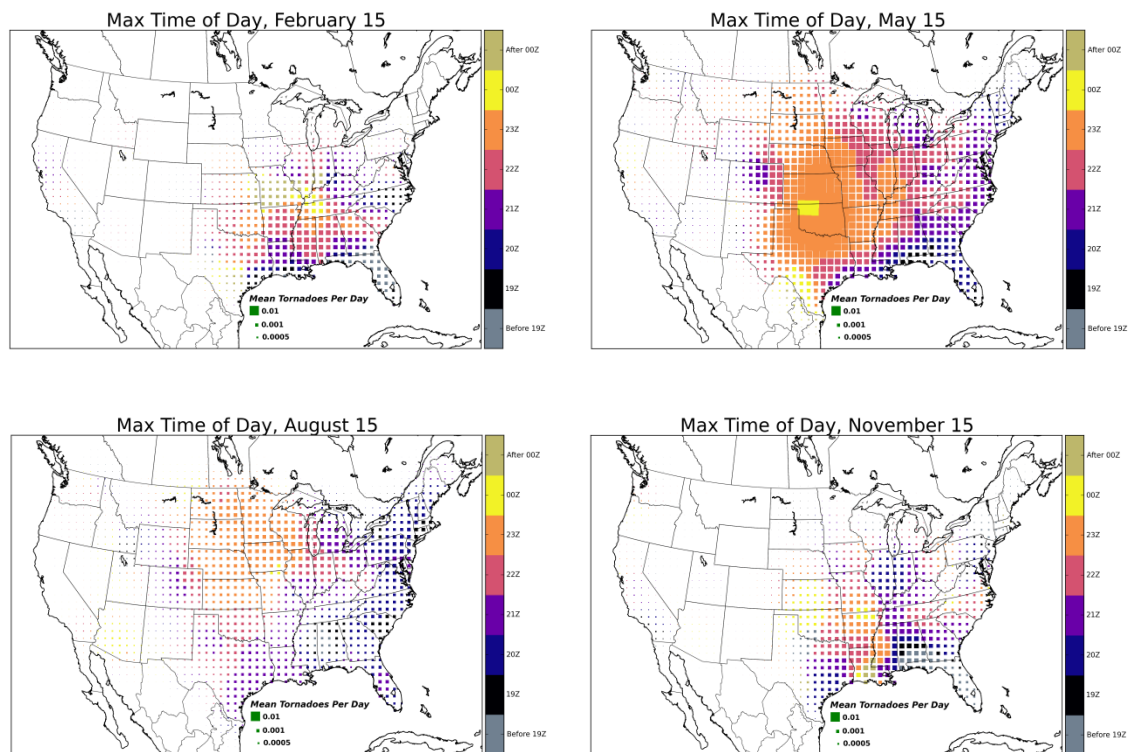
Figure 3.6: Mean tornadoes per day (represented by the size of the square) and peak
time (represented by the color of the square) for the 15th of February (top left), May (top
right), August (bottom left), and November (bottom right).

Additionally, the later peak hours are generally seen farther west, with the peak

hour becoming progressively earlier towards the east across the US. This can most

likely be attributed to the strength of the capping inversion, which is defined as the

relatively warm layer air aloft, usually several thousand feet above the ground, which

suppresses or delays the development of thunderstorms (National Weather Service).

Generally, the cap is stronger in the Plains than in the SE US, meaning that it takes

longer for daytime heating to generate enough energy at the ground to initiate

convection there. This generally leads to severe weather reports occurring later in the

Plains, and the pattern we see in the hourly climatology.

Finally, Figure 3.6 shows that the number of daily tornadoes (proportional to the

size of the square marker) is much more variable in the Plains than in the SE US. In all

four panels, the size of the marker remains relatively constant in the SE US, while the

August and February markers are drastically different in size in the Plains than the May

marker. This is consistent with the pattern shown in Figure 3.4; the Plains have a very

strong annual tornado cycle, with a peak in April and May, and the SE US does not

have a similarly strong cycle. However, while the SE US locations don't experience the

same magnitude in peak tornado frequency in any season, they often have a higher

number of daily tornadoes than the Plains, outside of the peak in the spring. This

indicates that on any given day outside of the April-June timeframe, states like Alabama

and Mississippi have a higher threat of tornadoes than Kansas and Oklahoma due to the

extreme peaked cycles in the Plains and the lack of any peak in the SE US. Not only

does this generally go against common perceptions of tornado risk, it also means that

the SE US needs to be prepared for these types of storms during all seasons. This is

analyzed later in this section.

To better visualize the locations of annual and daily peaks in tornado threat, heatmaps of all 8784 hours of the year were plotted for a number of locations. Figure 3.7 shows the heatmaps for Norman OK, and Huntsville, AL.
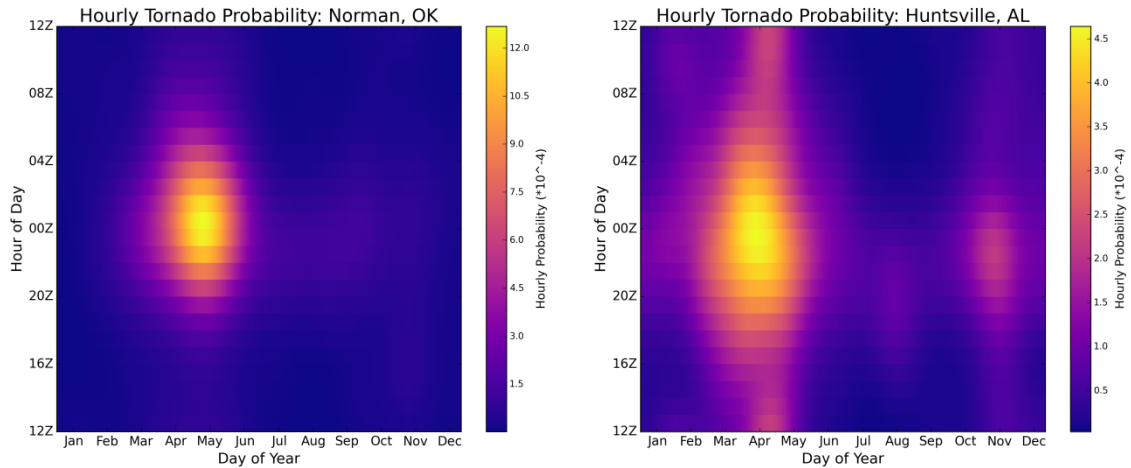
Figure 3.7: Heatmaps for Norman, OK (left) and Huntsville, AL (right). Note the color bars are not the same.

These two heatmaps exemplify the differences between the tornado threats in the Plains and SE US. The x-axis is the day of the year, and the y-axis is the hour of the day. The heatmap for Norman shows a single, very strong peak in the April and May between the hours of 20 UTC and 04 UTC. Beyond this timeframe, probabilities are extremely low, which indicates a very concentrated, specific season that tornadoes usually occur within. This supports previous findings in which more than 95% of all severe reports in a 24-hour convective outlook day occur within a 4-hour portion of that day. Huntsville, on the other hand, shows a very different pattern. While there is a relative maximum in probability in March and April from 20 UTC to 04 UTC, this maximum is about 40% of the maximum in Norman. Outside of this maximum, probabilities remain high relative

25

to the maximum. This indicates that the threat is spread across a much larger timeframe in the SE US than it is in the Plains, which has been shown in previous figures.

An application of the different tornado threats is the ideal community responses to these disasters. While one response model may work well in Oklahoma, Alabama residents will need to have a very different model to respond to threats that occur in very different times of the year. One example of this is related to the school day and school year schedule. Figure 3.8 shows the fraction of total annual tornadoes that occur during the school day. This proportion was calculated as 5/7 (since children are in school 5 of 7 days in a week) of the sum of the hourly tornado probabilities that occur between 7 am and 4 pm local time between August 15th and June 15th. The fraction of total annual hours spent in school is 0.198. There is a relative maximum in school day tornadoes in southern Alabama, southern Georgia, and the Florida peninsula. More than 25% of all tornadoes occur during the school day in these areas, whereas areas in North Dakota experience less than 5% of their total tornadoes occurring during the school day. These percentages align well with the hourly tornado probabilities for those areas shown in Figure 3.7. Proportions are higher where the daily and annual tornado cycles are less peaked, or where the peak occurs during the school day. The width of the tornado peak also manifests itself in these results. Those areas with a wider peak will have higher school day tornado occurrence, where areas with a lower width will have fewer tornadoes occur during the school day if the peak is in the late evening.

Figure 3.8: The fraction of total annual tornadoes that occur between 7 am and 4 pm local time between August 15th and June 15th.

This has major implications for how these schools prepare for such disasters. I know from personal experience that schools in Minnesota have tornado drills once a month throughout the entire year. While this may be sufficient for an area that sees few tornadoes and even fewer during school hours, other areas with a higher overall tornado risk and a higher number of tornadoes during school hours would likely need to have more frequent drills to keep both students and administrators aware of what protective actions need to be taken during the event of a tornado with children in the building.

Another notable trend in tornado probabilities is the location of the peak day (defined as the day of the year with the highest tornado probability). This day was found

for each year in the period (1955-2015), which allowed for the calculations of medians and interquartile ranges. This information gives insight into the different annual cycles in different regions, how variable those annual cycles are, and how the cycles have changed throughout the 61 year period.

Median Peak Tornado Day
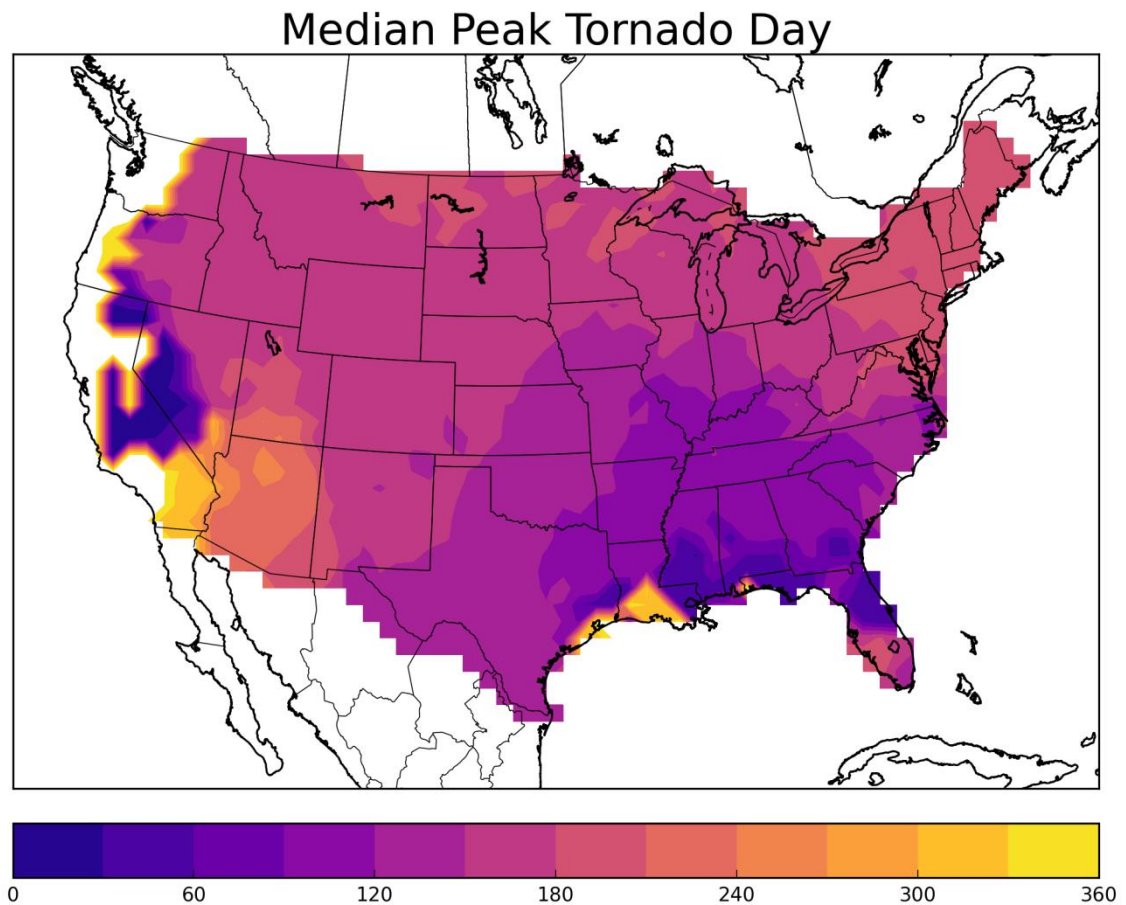
Figure 3.9: Median day of the year with the highest number of total tornadoes.

Since there are many points that have multimodal peaks-often one in the spring and one later in the year-some rearranging of the data points needed to be done before any mid-point calculations could be analyzed. The start and end points of the year needed to fall such that tornado seasons were not split by the January 1st/December 31st break point. Therefore, all peak days were gathered and then the interquartile range

(IQR, defined as the 75th percentile minus the 25th percentile) was calculated to understand the range of the primary dataset of peak days. Then days were sorted by number of the day it occurred (with January 1st being day 1 and December 31st being day 366). One by one starting with the lowest numbered day, 366 was added to the day number and then the IQR was re-calculated with the new, wrapped dataset. Once all 61 days had been wrapped and 61 IQRs were calculated, the minimum IQR was found, and that wrapped dataset was used to calculate the median peak day. Many points in the SE US needed 40-50 values wrapped, most likely due to the secondary tornado season occurring in November and December. Once the median peak day was calculated for all points, 366 was subtracted from any median over that value to re-orient the year back to days 1-366.

Figure 3.9 shows the median day of tornado occurrence for any point in the US. The results are consistent with previous findings in that portions of the Midwest and Northeast have later peak days (during the months of June and July) compared to locations in the Plains that have peak days generally during the month of May. Peak days become progressively early in the year as one moves to the SE US. There is a portion of southern Louisiana that actually has peak days at the very end of the year. This straddling of the beginning and end of the year in the southeast is likely due to the nearly complete lack of an annual cycle in the Southeast. Given the much more variable annual cycles seen in the SE US, peak days could end up occurring at nearly any time of the year. This is explored in more depth later in this section.
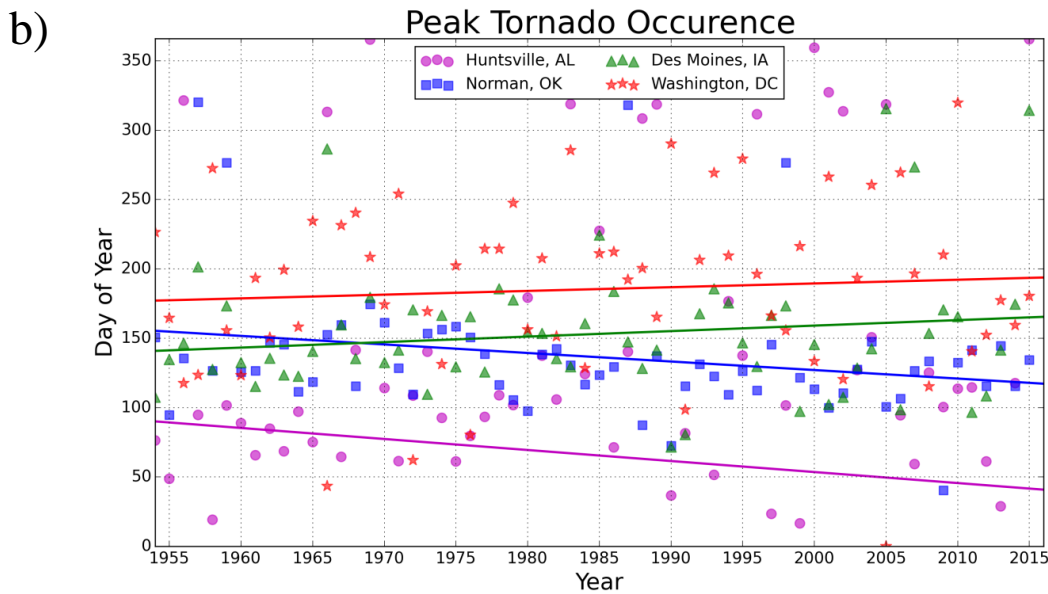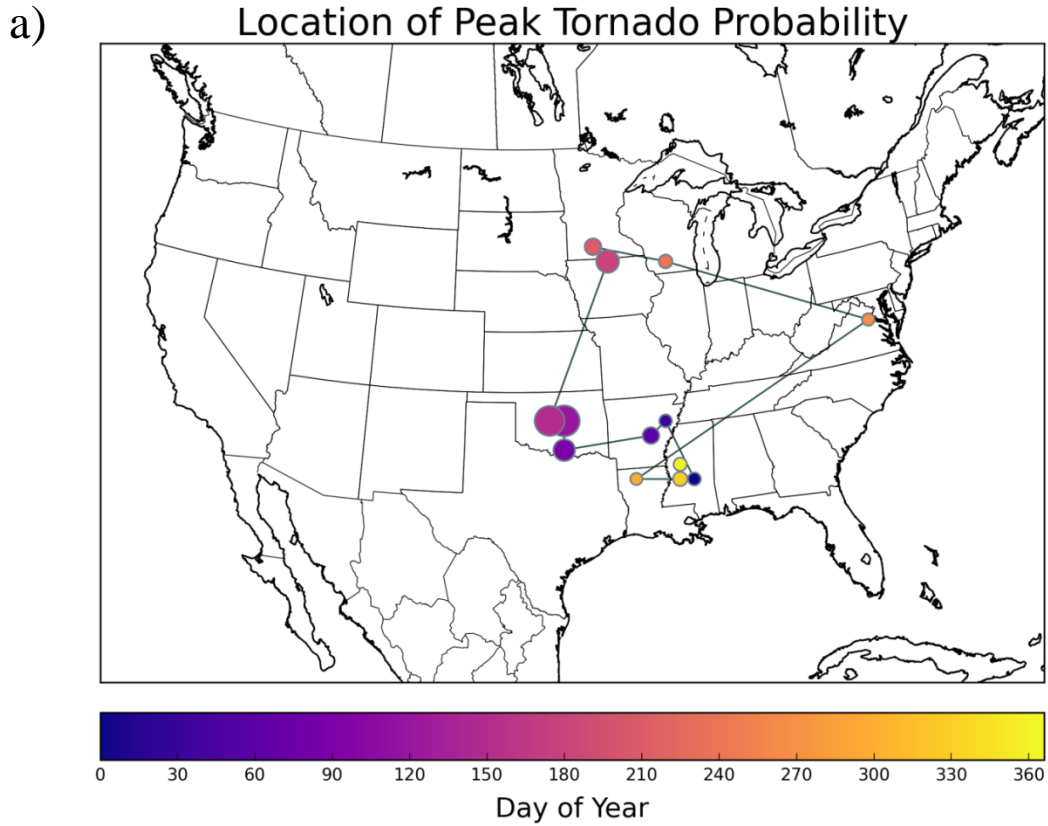
Figure 3.10: a) Location of peak tornado probability once every 30 days. Color of the point corresponds to day of the year the peak occurred; size of the point is proportional to the value of the maximum probability on that day. b) Peak tornado days per year for Huntsville, AL, Norman, OK, Des Moines, IA and Washington, DC. Solid lines are the linear regression of the peak days.

After looking at the peak for any location, we wanted to look at how the peak on each day changed location throughout the year. Not only did we want to understand how the peak changed location, but we also wanted to understand how that change in location also resulted in a change in magnitude. Therefore, the location of the peak was plotted on a map with the color of the marker representing the day of the year of the peak and the size of the marker being proportional to the maximum probability on that day. Figure 3.10a shows this figure with peaks plotted roughly once per month.

The first noticeable characteristic of the peak is the winter months are in the SE US. The colors bridge the colorbar, indicating the end of the year. Beginning in late winter and early spring, the peak moves from the Mississippi and Arkansas area into southern and central Oklahoma. This is when the most dramatic increase in marker size occurs. There is clearly an annual peak in tornado probabilities around this time, as none of the other markers are near the same size.

As the summer season progresses, the peak moves north into Iowa and Minnesota, similar to what was seen in the maps in Figure 3.6. Then there is a drastic shift in the peak location in the late summer and early fall, which moves the peak all the way to the east coast, before it moves back to the SE US for the cool season. This overall pattern in peak location exemplifies the annual tornado season, which has impacts everywhere east of the Rockies, from the SE US to the plains, to the Midwest states and all the way to the coast.

Next, we wanted to look at how the peak changed throughout the 61 year climatological period at each location. During the creation of the hourly climatology, we had to calculate the smoothed probability for each hour for every year, and then we

31

found the mean of those hourly values. This allowed us to compare hourly

climatological values across years and examine how they changed throughout the 61

year period. Although we showed earlier that the number of tornadoes has not changed

throughout the time period, we will now explore how the distribution of those tornadoes

has varied throughout the period.

Figure 3.10b shows the day of the peak tornado probability for each year in the

period at four different locations. The solid line is a linear regression of the peak days.

The regressions show the peak day becoming earlier in the year in Norman and

Huntsville, and later in Des Moines and Washington. In Norman, the linear regression

indicates that the peak day has become earlier in the year by 0.41 days per year. This is

very similar to the results from Lu et al. (2015), who found the peak day to decrease at a

rate of 0.37 days per year, but much larger than Long and Stoy (2014), who only found

a 0.12 days per year decrease. However, the Long and Stoy study did not specifically

find a decrease for central Oklahoma, but averaged the change over the entire Plains

region. Additionally, the authors acknowledge their method produces conservative

estimates for the change in peak tornado days. Next, some differences in the methods

could explain the lack of statistical significance of our peak day decrease over time. We

used a larger dataset (1955-2015 vs. 1979-2013) than the Lu et al. (2015) study and

used all data points, including some potential outliers with peak days after day 250.

Even though the regression slopes were not statistically significant, the regression lines

for both Norman and Huntsville have the most dramatic slopes. The later end of the

regression lines for these locations fall outside of the 95% confidence interval for the

mean peak day (Norman: [124.82, 148.99] and Huntsville: [49.18, 83.30]), which

indicates a 95% confidence that the mean peak tornado day has become earlier in the year throughout the time period.

3.3 The Peakedness of the Diurnal Cycle

Once the differences in the peak times and peakedness of both of the diurnal cycle and annual cycle were discovered, many more questions became evident. How do these patterns change spatially? Temporally? What implications do these differences have for community response to tornadoes? How should different communities respond to their specific threat? The following sections attempt to answer some of these questions and explore different methods for quantifying the peakedness of the diurnal and annual tornado cycles.

First, we looked at what the extremes in daily cycle peakedness looked like. What locations have the most different characteristics in daily and annual cycles, while still having similar overall tornado threat? Figure 3.11 shows the annual cycles for each
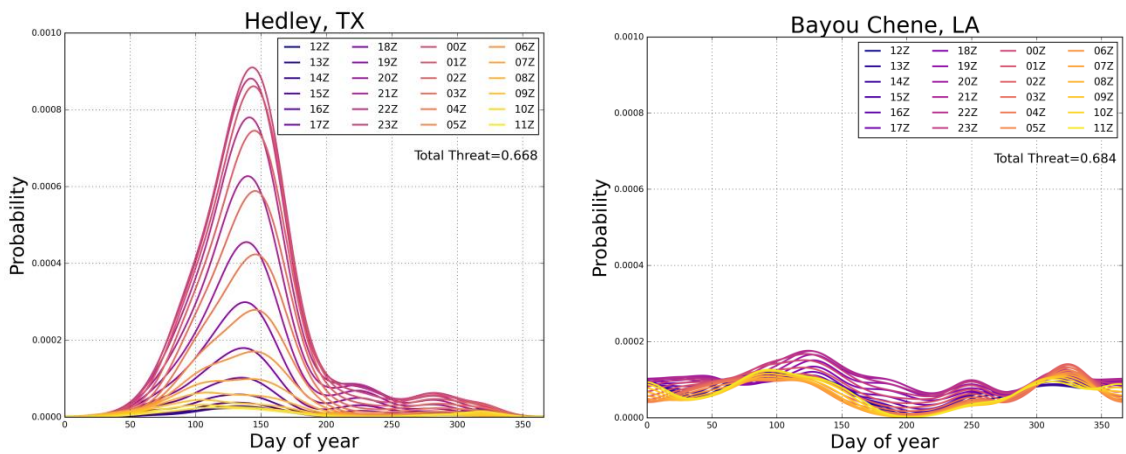
Figure 3.11: Hourly tornado probabilities at corresponding hours for each day of the year for Hedley, TX (left) and Bayou Chene, LA (right). Each hour is a different color. Total annual tornado threat is nearly identical for both locations.

33

hour of the day for two different locations. Each figure has 24 different lines on it, one for each hour. The hourly tornado probability during that hour for each day of the year was plotted. This was done to ensure both the annual and the daily cycle would be represented on a single plot.

The total annual tornado threat for Hedley, TX (east of Amarillo, Figure 3.11 left) and Bayou Chene, LA (southwest of Baton Rouge, Figure 3.11 right) are very similar (0.668 and 0.684, respectively). However, the distribution of that total threat is anything but similar. Hedley very clearly has an annual peak in tornado threat around day 140 (May 19th), whereas Bayou Chene has no distinct peak. One could argue that there is a relative peak around day 125 (May 4th), but this peak is around 25% of the magnitude of the peak in Hedley. To counter this high amplitude peak, the tornado probabilities outside of day 75 to day 200 (March 15th to July 18th) are very close to zero. This is not the case in Bayou Chene, where probabilities remain around 0.0001 or higher for most of the year.

In addition to the lack of an annual cycle in Bayou Chene, there also isn't much of a daily cycle either. The largest range in hourly tornado probability on a single day is about ½ of the largest value, whereas the largest range in Hedley is about 9/10 of the largest value. The 24 different lines (one for each hour) are widely spread in May in Hedley, which simply is not the case for any point in the year in Bayou Chene, where all 24 lines are much closer in magnitude.

The drastic differences in the distribution of a nearly identical total annual tornado threat exemplify the challenges many forecasters face in the SE US. For example, a forecaster working on a tornado forecast for the middle of May in Hedley,

34

TX would likely be able to identify a four to six hour period when tornadoes were most

likely to occur, without seeing any information about the synoptic setup or

environmental parameters. This is nowhere near the case for forecasters in Bayou

Chene because the climatological hourly tornado probabilities are very similar to each

other for every hour in the month of May (and the entire year for that matter). These

two sets of forecasters are working under very different background assumptions, which

pose different challenges for creating a forecast.

Similarly, responses by these communities could be equally as different. It is

very unlikely that Hedley residents would ever experience a tornado in February at 8

am, but this is a very possible situation for residents in Bayou Chene. Therefore,

Emergency Managers in these communities will need to have very different disaster

plans. Those in Hedley might have a single disaster plan for all tornadoes because

nearly all of the events they experience are in the afternoon during the late spring and

early summer months. Those in Bayou Chene might need multiple disaster plans for

tornadoes: one for winter events, one for spring events, one for school hours and one for
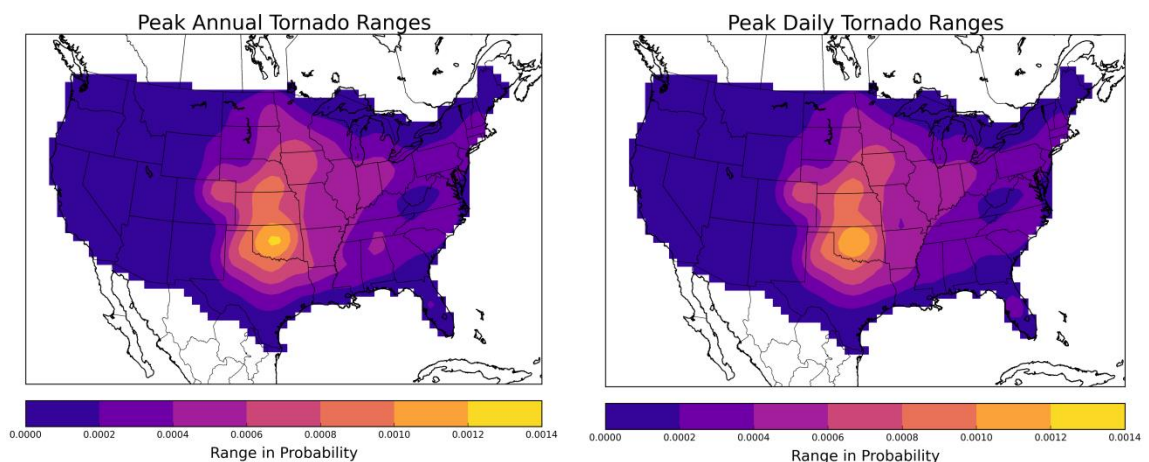
Figure 3.12: Maximum annual (left) and daily (right) ranges in hourly tornado
probabilities.

rush hour traffic. Ultimately, the differences in both the annual and daily cycle of climatological tornado risks requires both scientists and communicators to be aware of how the risk at their location impacts residents and property.

Another measure of the peakedness of a cycle is the magnitude of the range of daily and annual probabilities. The maximum and minimum value of both the annual and daily cycles of hourly tornado probabilities were calculated, resulting in the peak range at each location. These values equate to a measure of how peaked a cycle is. For example, locations with smaller ranges have a flatter cycle because the maximum and the minimum values are closer together, while those with larger ranges have a more peaked cycle because the maximum and minimum values are farther apart. Figure 3.12 shows these values for the annual range (left) and the daily range (right).

These plots are nearly identical, indicating that the maximum and minimum probabilities often occur on the same day. The maximum in both annual and daily range occurs in central Oklahoma, with a very sharp gradient to lower values moving south into Texas and east into the Arkansas and Louisiana areas. Annual and daily ranges in the SE US are 1/6 to 1/7 of the magnitude of the ranges in central Oklahoma. These results align well with previous plots work showing the peaked cycle in the Plains and variable cycle in the SE US.

In addition to the range of the peaks, the interquartile range (IQR, which is the 75th percentile minus the 25th percentile) quantifies how much spread there is within the middle 50% of the data. Points with a larger IQR have flatter cycles because the data points are spread over a larger range of values than points with a smaller IQR. One benefit to using the IQR over the range is that the IQR is resistant to outliers. Therefore,

points with one or two years with a much later or earlier peak than all the rest will not see large changes in the IQR due to those anomalous years.

The same process described in section 3.2 for the calculation of the median peak day was used to calculate the IQR of the peak days. The peak day for each year was calculated, and then 366 was added to those day numbers one by one starting with the lowest numbered day. Each time this was done, the new IQR was calculated and the dataset with the minimum IQR was used for any further calculations. This process ensured that tornado seasons that spanned the December 31st/January 1st breakpoint

![IQR of Peak Tornado Days map of the continental United States with a colorbar ranging from 20 to 140]
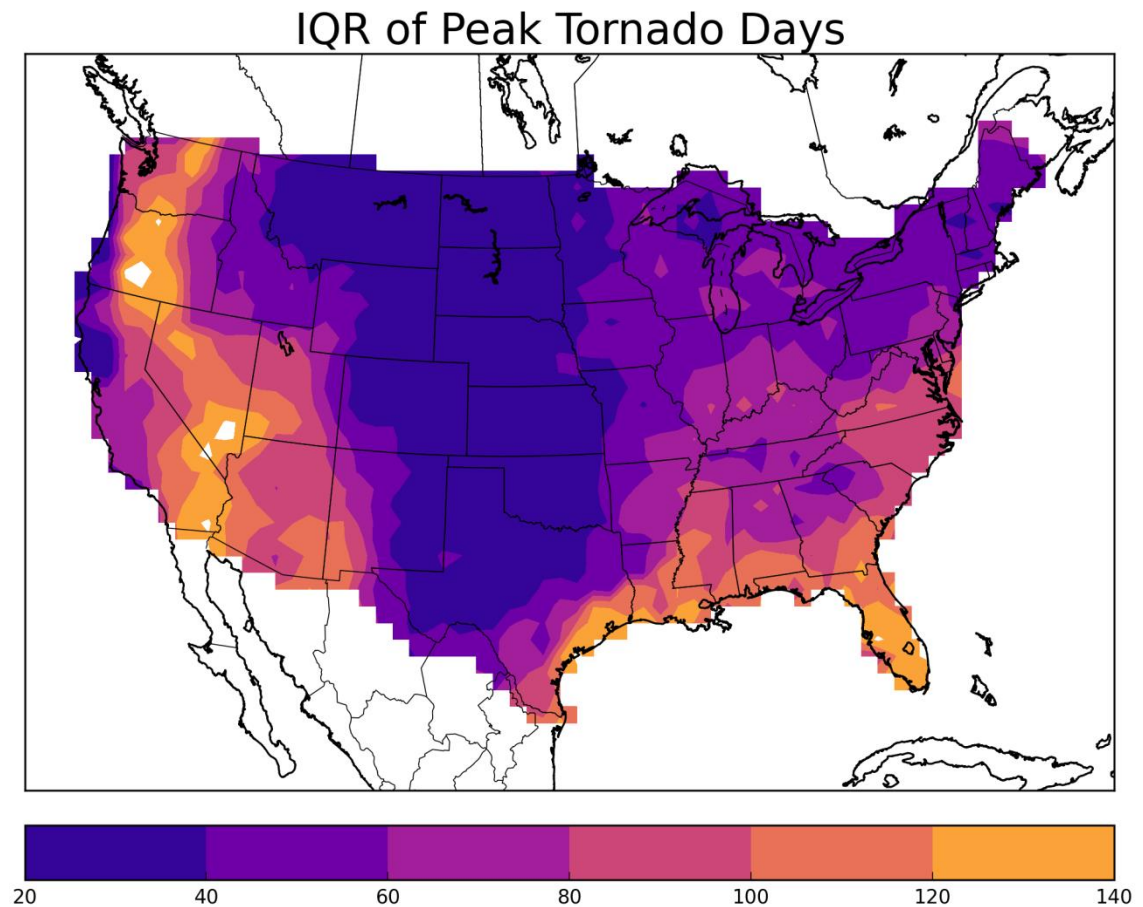
Figure 3.13: The interquartile ranges of the climatological tornado peak days from 1955-2015.

were not arbitrarily split in half and the middle values calculated as sometime in June.

Figure 3.13 shows the IQR values for all points across the US. The most notable

characteristic of the IQR pattern is the very low values over and to the east of the Rocky

Mountains. The values in this area indicate that the peak day for tornadoes has been

very constant over the 61-year period. Additionally, it would also indicate that the

tornado season is concentrated within a couple months, as the peak day does not vary

much from year to year. The gradient of the IQR values is another characteristic to note.

In the northern portion of the country, the gradient of the IQR values is very weak or

near zero. However, the gradient from the southern plains to the SE US is very strong.

This indicates the climatological tornado risk is less peaked in the northern portion of

the country, but still follows the same general pattern, whereas the SE US does not

adhere to the same pattern. It is much more variable in both length of the season and in

peak of the season.

3.4 Sub-daily Tornado Threat Periods

Previous work showed that a majority (about 97%) of severe reports occur

within a small portion of the day. This was discovered by gathering all severe reports at

a single 80 km grid point and then calculating maximum percentage of daily reports that

occurred within 4-hours. Given that a large majority of daily reports fall within a 4-hour

window, we wanted to understand how the timing and duration of said window behaved

on a climatological scale.

We quantified the peakedness of the climatological daily cycles by calculating

the maximum percentage of the total threat enclosed in a four hour period. For example,
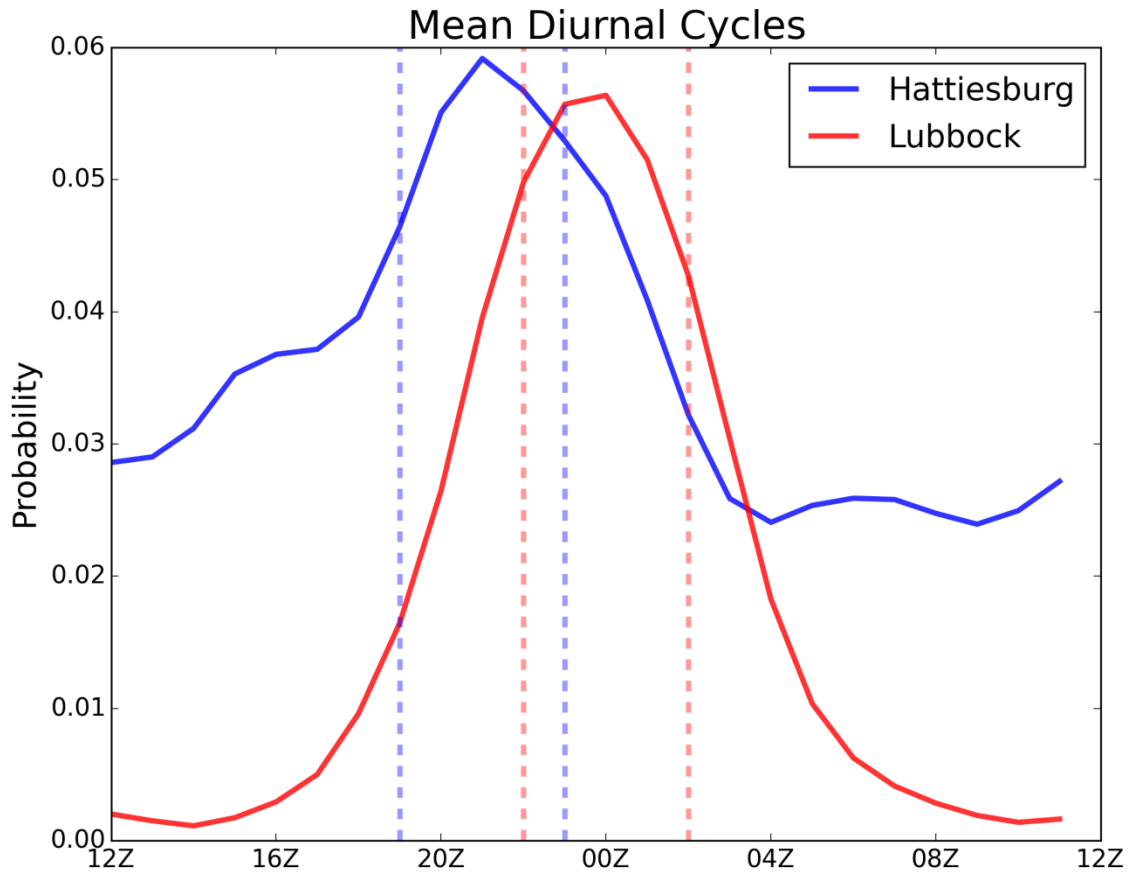
Figure 3.14: Mean daily tornado cycle for Hattiesburg, MS and Lubbock, TX. Dashed lines represent the start and end of the four hour period enclosing the largest area under the respective curves.

if a cycle was completely flat, the percentage captured should be about 16.7% (4 hours / 24 hours). Therefore, the higher the percentage captured, the more peaked a cycle is. Figure 3.14 shows the mean daily cycle for Hattiesburg, MS and Lubbock, TX. The area under the curves represents the total daily threat for tornadoes, and the dashed lines represent the beginning and end of the four hour period enclosing the largest area under the respective curve.

While the maximum area encompassed in a four hour period may look very similar, or even larger for Hattiesburg than for Lubbock, the higher hourly probabilities

outside of the peak four hours in Hattiesburg means the total area under the curve for

Hattiesburg is much larger than that for Lubbock. This means that the ratio of the area

encompassed by the four hour period divided by the total area under the curve will be

larger in Lubbock than for Hattiesburg. Therefore, the larger the ratio, the more peaked

the daily cycle is.
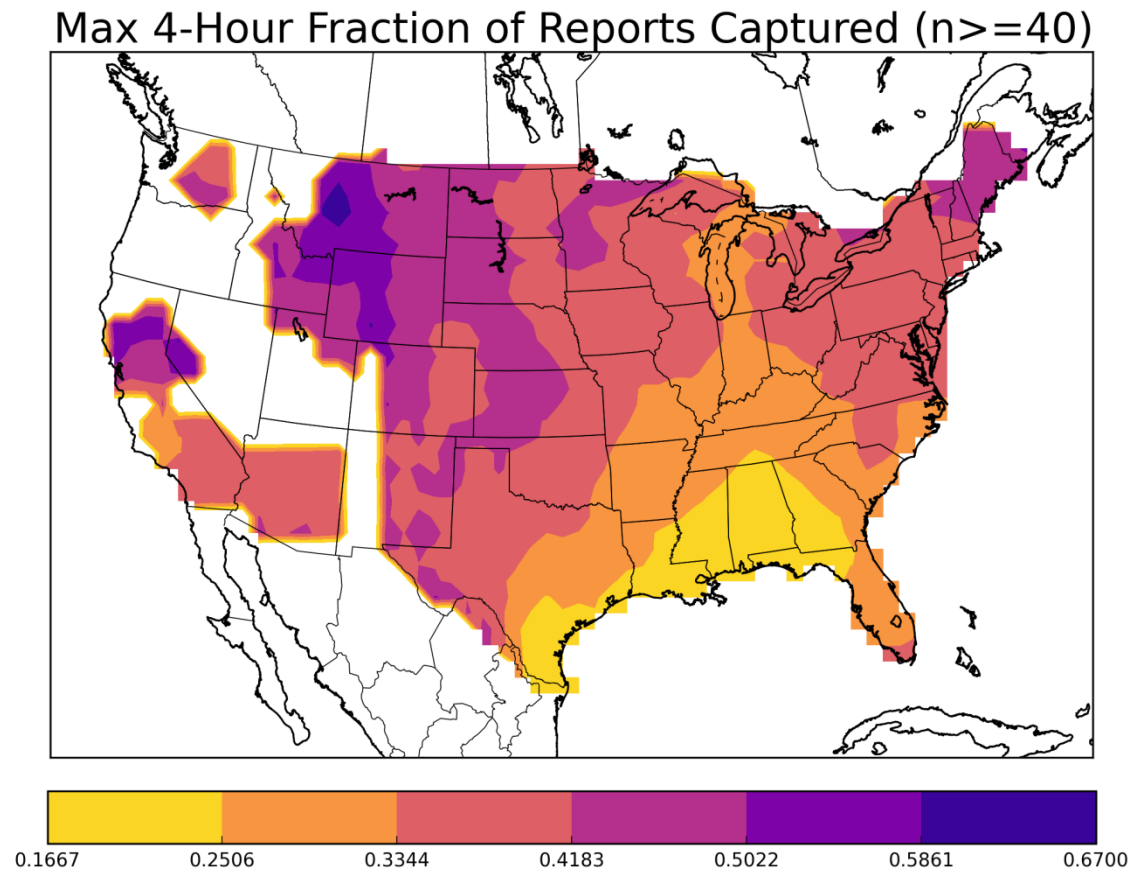
Figure 3.15: The maximum fraction of the total number of daily tornadoes captured in a four-hour period. Each point needed a total of at least 40 reports between 1955-2015 to have the fraction calculated.

This ratio can be calculated for all points in the US, but we chose to only

calculate it for those points that had greater than 40 tornado reports within the time

period. Figure 3.15 shows those ratios plotted across the US. Notice many locations

west of the Rocky Mountains have no data plotted due to the threshold imposed upon the calculation.

The most notable pattern in Figure 3.15 is the decreasing trend to the south and east from the Plains. Nearly half of all daily tornado reports are captured in a 4-hour period in portions of Texas, Oklahoma, Kansas, Nebraska and the Dakotas. On the opposite end of the spectrum is Mississippi, where nearly all of the state sees less than 25% of their daily tornadoes in a 4-hour period. Additionally, it is important to note that this calculation was done with a single 4-hour period for the entire year, i.e. the period did not change with the season, synoptic pattern, or the environmental conditions like we allowed it to in our first calculation. Outside of all of these factors, it is quite remarkable that nearly half of all tornadoes occur in the same 4-hour period each day in portions of the central plains. Given that 1/6 of all reports (about 0.1667) would occur in a 4-hour period if they were uniformly distributed, the low values in the SE US show the extent to which there is little diurnal cycle to tornado occurrence in these areas. This finding has a significant impact on how forecasters handle tornadic events in different areas of the country. There are some regional challenges that need to be addressed before we ask forecasters to create probabilistic information for tornadoes in the SE US. A forecaster in the plains in the early afternoon in May likely wouldn't need to know much about the synoptic weather pattern to know that she should be worried about the potential for tornadoes. However, outside of this annual and daily peak, that forecaster probably doesn't worry about tornadoes on any given day. Conversely, that same forecaster in the SE US would need to constantly be aware of the changing conditions to know whether or not tornadoes are possible because there generally isn't a

41

"high" and "low" season to these events. Training and time management strategies are going to be very different for forecasting tornadoes in these two regions. This measure showed one of the clearest differences between the Plains and the SE US with regards to how the diurnal tornado cycle varies spatially across the country.

After examining the peakedness of diurnal cycles across the country, the next step was to find when the most peaked times occurred at each location.

Start Time of 4-Hour Max Window (n>=40)

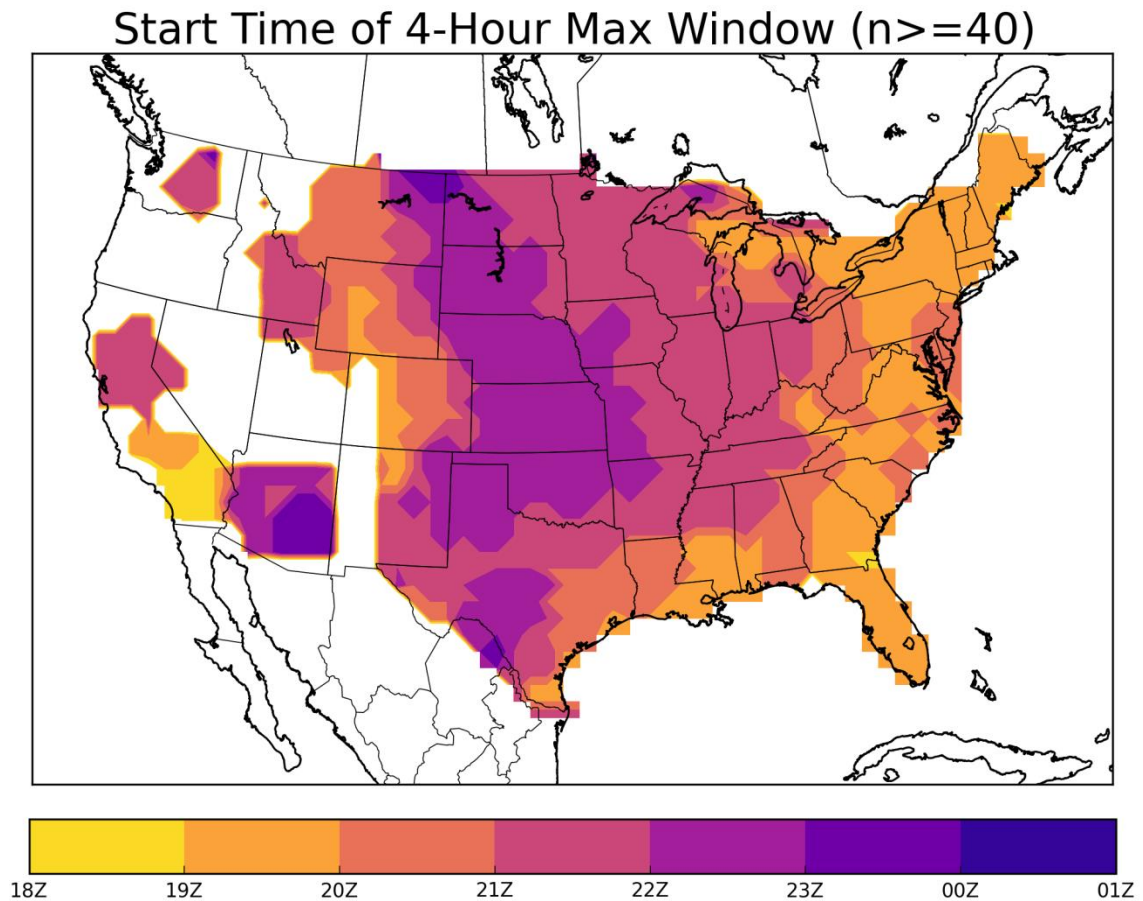Figure 3.16: Start time of the four-hour period that captures the highest fraction of tornado reports for every location across the country. Note the calculation was only done for points with greater than 40 reports over the 1955-2015 period.

While the implications of that threat timeframe are very different depending on which part of the country it is, the timeframe is still the climatological 4-hour period within

which the most tornadoes occur. Figure 3.16 shows the map of the start time for the 4-hour period at each location. The general pattern shows an earlier start time to the 4-hour period on the East Coast than in the Central Plains. Start times in the eastern part of the country are as early as 19 or 20 UTC, whereas most of the start times in the Plains are between 21 and 22 UTC. This aligns well with the results found in Figure 3.6, where the darker colored markers (corresponding to earlier start times) were generally restrained to the eastern part of the country, with the brighter colors corresponding to later start times were largely found in the plains states.

Both Figures 3.15 and 3.16 again highlight the important differences between the tornado threats in the Plains versus the threat in the SE US. First, there is a much more condensed timeframe for the climatological tornado occurrence in the plains states than in the SE US. This condensed timeframe makes the forecasting challenges in the Plains much different than those in the SE US. Next, the differences in start time of the maximum 4-hour period have implications for both forecasting and response. The maximum period in the Plains is generally in the late evening hours, after most people have gone home from work or school. The SE US has to respond to these events during the end of the school and work day, rush hour traffic and dinner time. These results are similar to those shown by Figure 3.8, where there are more tornadoes during the school day in the SE than in the Plains. The earlier start time of the 4-hour period shifts the tornado threat to coincide with school hours in the SE, which means that emergency preparation also needs to be different for the two areas. Children and educators need to be aware and proficient in their emergency response plans in the SE, whereas it is somewhat less of a concern in the Plains and especially in the northern Plains. These are

43

important differences to understand so that forecasters and emergency responders can work together to make region-specific disaster plans.

Another way to quantify the peakedness of the diurnal cycle is by calculating the number of hours needed to capture 50% of the total annual tornado threat. This was done by ordering all 8784 hours at each grid point from smallest tornado probability to largest. Then, starting from the largest probability, hourly probabilities were added together until the sum equaled 50% of the total tornado threat. The number of hours summed to be greater than or equal to half of the threat was then divided by 8784 to find a ratio of the number of total hours needed. Figure 3.17 shows the map for these ratios.
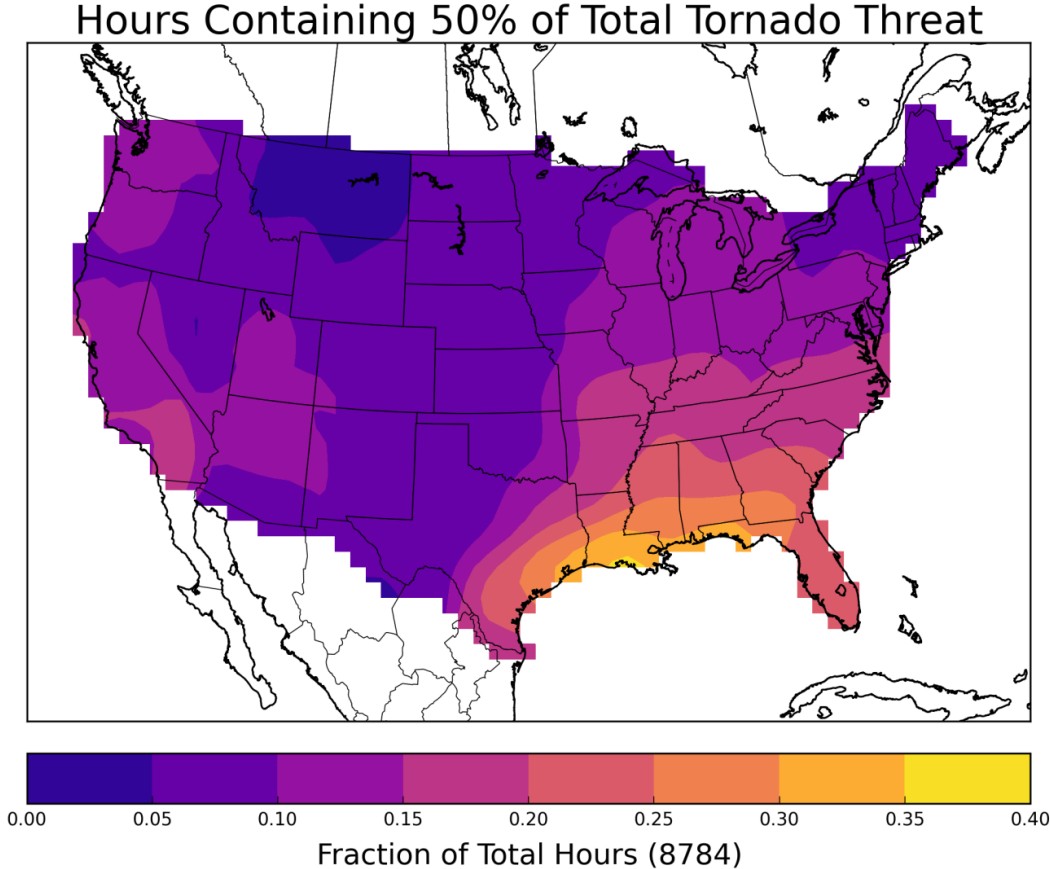

Figure 3.17: Fraction of total hours needed to capture 50% of the total annual tornado threat.

These results are similar to those found in Figure 3.15, with high ratios in the Plains and much lower ones in the SE US. One of the biggest differences between Figures 3.17 and 3.15 is the restriction to four consecutive hours in Figure 3.15, with no restrictions on what hours are used in Figure 3.17. This method uses the hours with the maximum probability, regardless of what day or hour they occur within. We were simply trying to quantify how concentrated the tornado threat is, whereas figure 3.15 shows how peaked the daily cycle is. Using both of these plots, we can see that both the daily and annual cycles are peaked in the Plains and the Midwest. However, the very steep gradient from the southern Plains into the SE US indicates that not only is the SE US daily cycle not peaked (see Figure 3.15), but neither is the annual cycle. There are areas in the SE US that have half of its tornado threat in 30-40% of the total hours. Again, this implies that there simply isn't a climatological "peak" in tornado probabilities, which makes forecasting and preparing residents for these events much more difficult than in the Plains.

There are certain locations in the eastern part of the country like Washington, D.C., Maryland, New Jersey and Pennsylvania that have similar maximum 4-hour tornado fractions as central Oklahoma, but have slightly higher fractions of total hours containing 50% of the annual tornado threat. These discrepancies distinguish the differences between the annual and diurnal tornado cycles. The diurnal cycle is just as peaked and consistent in the peak throughout the entire year in the Plains as out east (indicated by similar values in Figure 3.15), but the annual cycle is not as peaked in the east as it is in the Plains (indicated by the slightly higher fraction of hours in Figure

45

3.17). Distinguishing factors like these are important in understanding differences in

forecasting methods and philosophies.

Finally, another way to look at the peakedness of the diurnal cycle throughout

the year is to plot the difference of the maximum and minimum probability on each day.

This was done for all 366 days at each point by finding the maximum and minimum

values between 12 UTC and 12 UTC for each day and then subtracting those values.

Therefore, larger differences in probabilities indicate a more peaked cycle for that day.

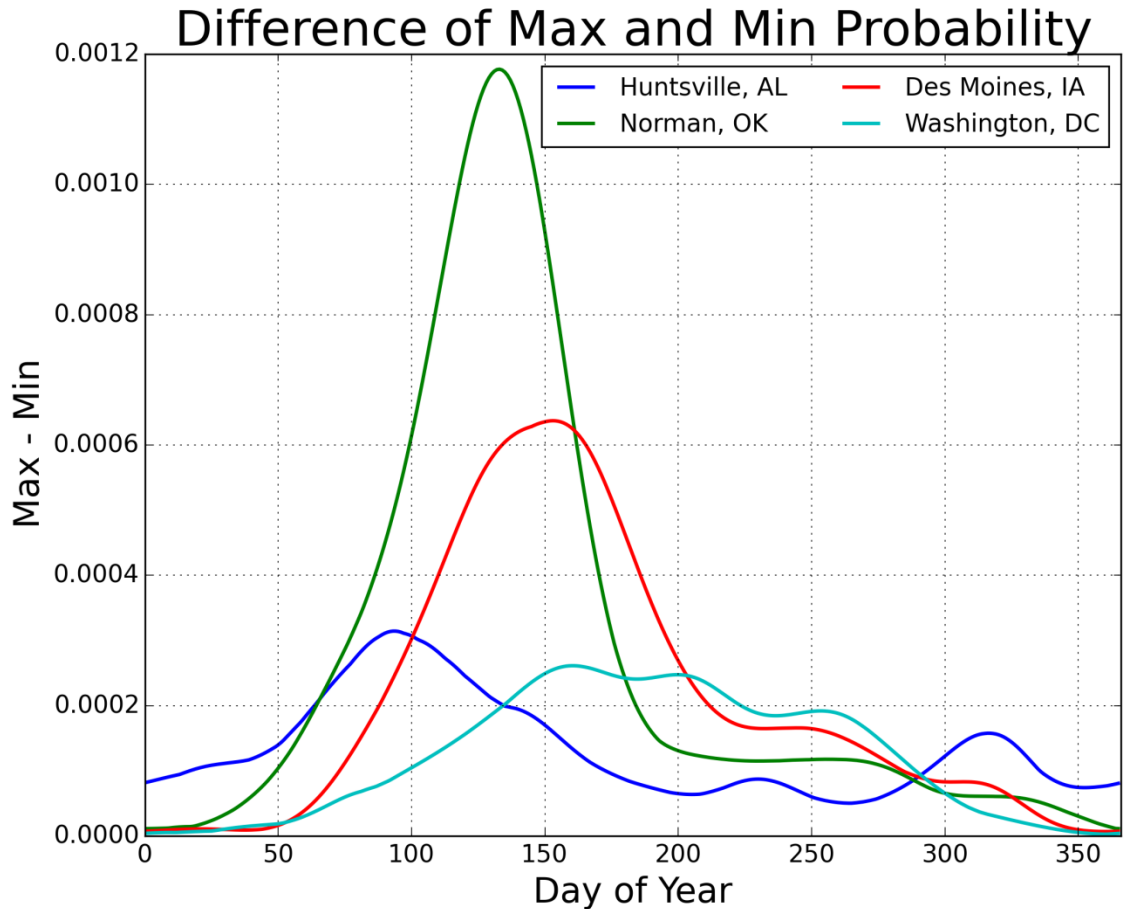However, very large differences could also be due to the lowest value being effectively

Figure 3.18: The daily maximum minus the daily minimum probability for each day of
the year for four locations across the country.

zero, which is particularly possible for locations in the southern plains as many days outside of March-June often have a near zero tornado threat. The daily differences were plotted in Figure 3.18 for each day of the year for Norman, OK, Huntsville, AL, Des Moines, IA, and Washington, D.C.

The four locations were chosen because they represent four very different parts of the country with respect to the climatological tornado threat. Des Moines and Norman are the most similar in terms of shape of the daily differences. There is a peak in the spring or early summer months, indicating the daily threat is very peaked during these months. The difference decreases and plateaus in the fall before decreasing again to nearly zero during the winter. The constant differences in the fall are likely due to very low magnitude maximums but near zero minimums on those days.

The Huntsville and Washington areas are drastically different in regards to the differences in daily tornado probabilities throughout the year. Huntsville has a very marginal peak in the daily difference around the beginning of April and then a secondary peak in November. While the overall values never even reach 1/3 the magnitude of the Norman differences, they also don't get as low as the Norman values either. These much more constant values again exemplify the lack of either a daily or an annual cycle in the SE US. The daily differences in Washington exhibit a similar pattern but almost opposite in time of the year compared to Huntsville. There is a very obvious decrease in daily differences during the summer months in Huntsville, which corresponds very well to the maximum in daily differences in Washington, D.C. This may indicate the peaked values in tornado probability moving north during the summer before the secondary cool season increases tornado probabilities in the SE US again in

the fall. While the differences in tornado probabilities are very low in Washington, D.C., they are generally restricted to half of the year, whereas the SE US differences never reach zero and peak during multiple times of the year. Simply having a concentrated peak is one pattern, having a less concentrated peak is another, and then having a non-existent peak, or a variable pattern is an entirely different phenomenon specific to the SE US.

Throughout this chapter, we have explored the characteristics of hourly tornado probabilities, total daily and total annual tornadoes, and how the annual and diurnal cycles vary in both space and time. These characteristics were highlighted because of the unique ability to analyze tornado probabilities on a sub-daily scale. The variations in the diurnal tornado cycle are crucial to understanding how forecasters, emergency managers and community members should create, disseminate, and respond to tornado threat information on a sub-daily scale. Regional differences in the daily distribution of the tornado threat are going to create unique challenges to communities in different parts of the country. This is something that needs to be carefully understood and integrated into any new forecast systems created in the coming years under the FACETs paradigm. Next, we attempt understand the same variations across the country, but this time for severe hail events.

Chapter 4:Characteristics of Hourly Hail Probabilities

4.1 Distribution of Hourly Hail Probabilities

There were many more challenges to working with the severe hail reports than there were when working with tornado reports. One of the biggest challenges is the exponential increase in overall hail reports and linear increase hail grid point days. After attempting to correct for the reporting practice changes seen in the dataset, we looked at the distribution of hail events across the US on a sub-daily scale. After gridding and smoothing all reports larger than 1.25 inches on an 80 km grid, we found the magnitude of the total annual hail threat for any point in the US. We added all 8784 hourly
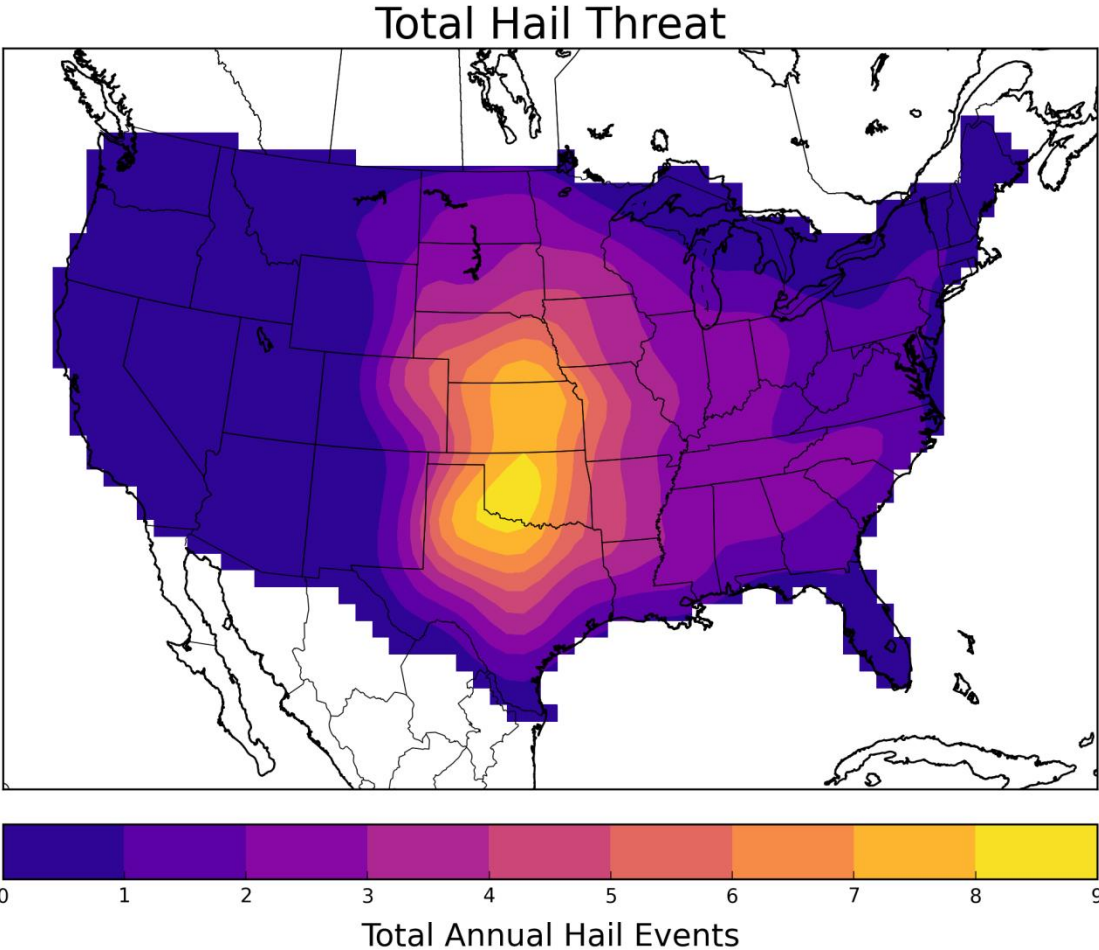

Figure 4.1: Total number of annual hail events for all points across the US.

probability values together for each grid point and then plotted the results, which can be

seen in figure 4.1. There is a peak in southwestern and western Oklahoma, with a very

sharp gradient to the southwest into Texas and westward into the Texas panhandle. The

8-9 event peak in Oklahoma gradually tapers off to the east to a minimum of 1-2 events

in the southern Alabama and Georgia regions. The SE US regions that had nearly the

same magnitude of annual tornado threat as Oklahoma (seen in Figure 3.1) only

experience about 1/3 of the hail events. This highlights the important differences in

typical regional lapse rates and convective mode between the two areas. The lack of

annual hail events with nearly equal annual tornado events indicates that the lapse rates

in the SE are much less steep than in the Plains, meaning there is less Convective

Available Potential Energy (CAPE) in the SE, which produces weaker updrafts in

storms. These weaker updrafts aren't able to loft hail as high into the atmosphere,

limiting the size of hail that can occur. This difference also indicates that tornadoes

occur in storms that produce a large amount of hail in the Plains, and in storms that

don't produce much hail in the SE. Not only does the SE US see tornadoes at any time

of the year and any time of the day, but Smith et al. 2012 found that those tornadoes

displayed the greatest variance in storm type, from discrete, right-moving supercells to

quasi-linear convective systems. This work also found that most significant hail events

occurred in the Plains, which is likely a manifestation of the lapse rate variations

between the two regions. Additionally, Trapp et al. (2004) found that tornadoes from

linear systems are much more common in the winter than cellular modes. Therefore, the

secondary tornado season in the winter in the SE US is more likely comprised of linear

mode storms that produce less hail. All of these results are easily seen in the hourly

climatology of reports we have produced.

Similar to the tornado climatology, the hourly hail climatology shows very

similar daily hail threats across adjacent days, but very different hourly hail

probabilities within those same days. Figure 4.2 shows the total hail threat for May 15th

and May 16th. While the magnitudes of the hail and tornado threats are obviously very

different, the distributions of the threats show some interesting characteristics. The

peaks in climatological tornado and hail events align very well with each other in the

central and southern Oklahoma areas. The higher probability plume for tornadoes

spreads farther east than the hail threat does, indicating that the hail threat has a smaller

area of influence relative to the tornado threat. However, the same pattern in similarities

between adjacent days seen in the tornado threat still holds for the hail threat. Both

maps in Figure 4.2 are very similar to each other, which is what we expected.
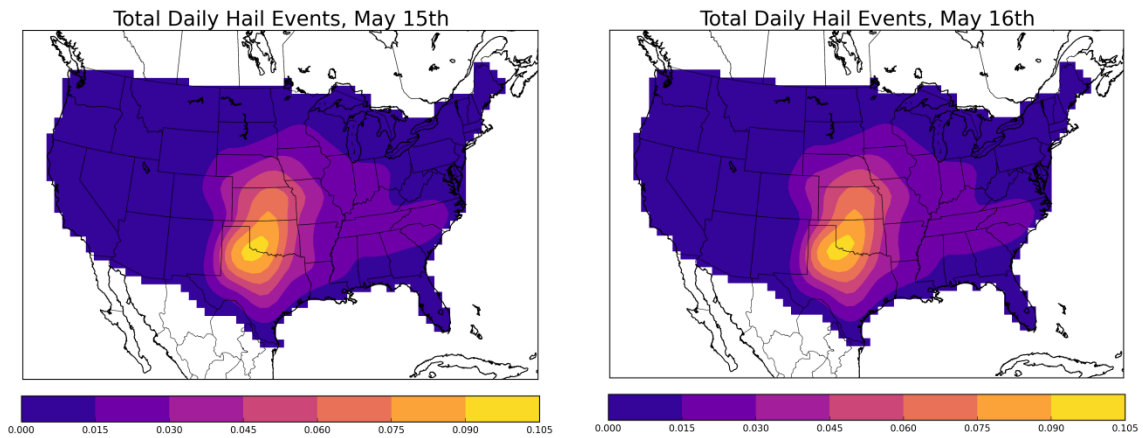

Figure 4.2: Total daily hail events for May 15th (left) and May 16th (right).

While the total daily hail events is nearly identical for adjacent days, the hourly

probabilities that make up that total daily threat are very different from each other.

Figure 4.3 shows the hourly hail probabilities for May 15th at 10 UTC (left) and May

15th at 22 UTC. It is important to note that the color bars are different by an order of magnitude, such that all the probabilities on the left map are represented by the darkest color on the right map. The general area of the peak probabilities is similar for both the morning and the evening hours, which indicates that most areas follow the diurnal cycle and are at least somewhat peaked. This is in contrast to what was seen with the tornado probabilities, where the SE US had a similar magnitude peak to the southern Plains in the morning, but then had a drastically lower probability in the afternoon. The only notable difference between the morning and afternoon graphics is the magnitude of the threat, which can be attributed to the diurnal cycle.
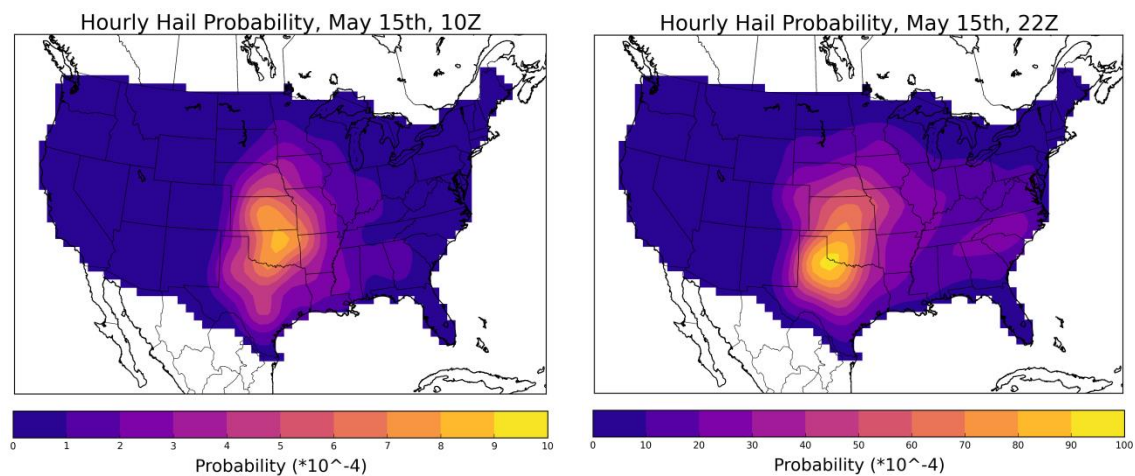
Figure 4.3: Hourly hail probability at 10 UTC on May 15th (left) and 22 UTC on May 15th (right). Note the color bars differ by an order of magnitude.

Next, we decided to once again look at the annual and daily ranges in hail probabilities, similar to what was looked at for tornado probabilities. Figure 4.4 (left) shows the difference in the annual maximum and annual minimum probability for each point across the country. These could be any hour of the year, as there was no restriction on when the values occurred. The right map in Figure 4.4 shows the largest difference between the maximum and minimum daily probability. The only change from the left

52

graph is that now we required the two values to occur on the same day. Similar to what was seen with the tornado probabilities, the two maps are very similar. However, there is a larger maximum in the annual range in the southeast Texas Panhandle than in the daily ranges. Generally, the annual maximums are slightly higher in the areas where the values differ, which indicates that the largest values in hail probabilities don't necessarily occur with the greatest diurnal peaks. This result differs from the tornado ranges, which were nearly identical for both the annual and daily ranges.
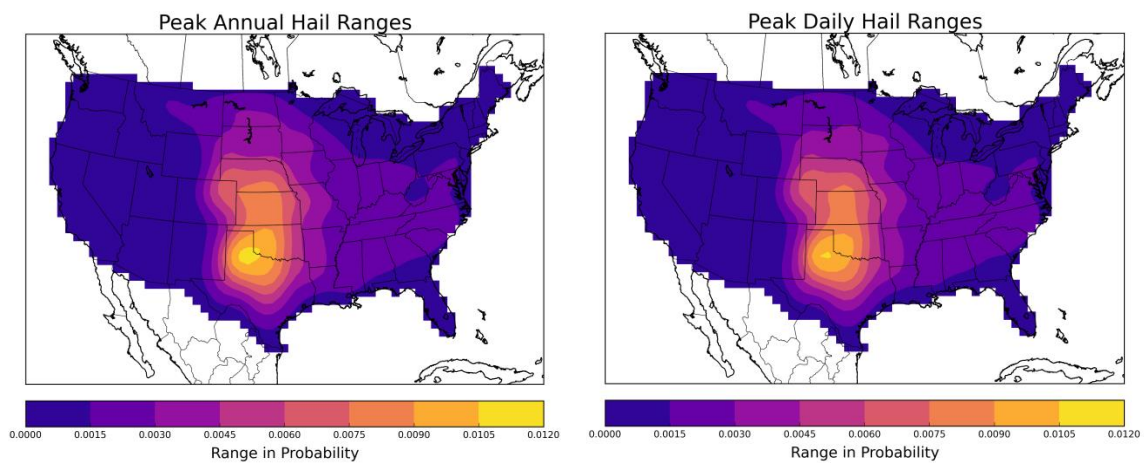
Figure 4.4: Maximum annual (left) and daily (right) ranges in hourly hail probabilities.

Further investigation of the distributions of hail probabilities show a more variable pattern in the SE US, but not nearly the same magnitude difference we saw with the tornado probabilities. Figure 4.5 shows line plots for each hour of the day, for all 366 days of the climatology, for Hedley, TX and Bayou Chene, LA. This is similar to Figure 3.11, except now the probability values are for hail events instead of tornadoes. The most noticeable difference between these plots and the tornado plots is that there is a peak at both locations throughout the day and throughout the year. Note that the y-axes differ by nearly an order of magnitude. While Bayou Chene doesn't

show as much of a peak in the diurnal cycle (probabilities are still relatively high

overnight), there is certainly more of a peak to the hail probabilities than there is to the

tornado probabilities. Similar to the tornado probabilities in Hedley, the hail

probabilities are also very peaked. Overall, this shows that hail events are both

seasonally and diurnally dependent in all regions of the US, which is very different

from tornadoes.

The majority of the hail threat in Hedley is contained within 125 days of the

year, whereas the majority of the threat in Bayou Chene is contained in 150-200 days of

the year. This means that forecasters and community members in Hedley generally only

need to be aware of hail events for less than half of the year, where Huntsville needs to

be aware of this threat for nearly 60% of the year and for nearly all hours of the day.

While this difference may not seem noteworthy, it can have a large impact on

forecasting philosophies. For example, forecasters for Bayou Chene operate under very

different background climatology information than forecasters in Hedley do (i.e. a

generally spring and early summer hail season versus a January-September hail season).
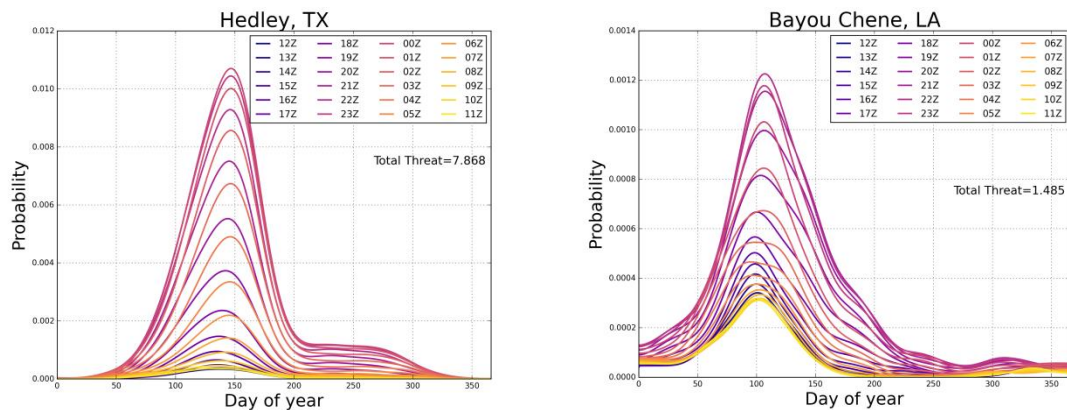

Figure 4.5: Hourly hail probabilities at corresponding hours for each day of the year for Hedley, TX (left) and Bayou Chene, LA (right). Each hour is a different color. Note the y-axis scales are different.

These differences are also extremely important for emergency managers who try to prepare their communities for all forms of hazardous events throughout the year.

4.2 Peakedness of the Annual and Diurnal Hail Cycles

After looking at the general distribution of the hourly hail probabilities, it became apparent that while there were many similarities between the tornado and hail probability distributions, there were also some notable differences. To further understand the differences between the annual and daily distribution of the hail threat, we plotted the same heatmaps as in Figure 3.7 for both hail probabilities for Norman, OK and Huntsville, AL. Figure 4.6 shows these plots with different color bar ranges for the two locations. The most obvious deviation from the pattern seen in the tornado probability heatmaps is the more diffuse cycle in Norman. The peak in hail probabilities extends from before 20 UTC in the afternoon until nearly 08 UTC during the overnight hours. Additionally, these higher probabilities span the months of March through June. When this area is compared to the shorter April-May tornado season with the hours of peak probability between 20 UTC and 04 UTC, it is obvious that the hail season is longer and has a more diffuse daily gradient. Interestingly, an additional secondary season can be seen in late August until the beginning of October. Although the magnitude of those hourly hail probabilities are much smaller than in the spring, there is a noticeable increase from the off season values.

The Huntsville hourly hail probabilities are different in many ways from the tornado probabilities in Norman. Huntsville's hail season is much more concentrated than the tornado season, with distinct "off"- hours and off-season values. While the

55

higher hail probabilities span the end of February until the end of June, the values

outside of that season are remarkably low relative to the high probability season

compared to the off season values in tornado probabilities. This is another indication

that while most tornado reports in the Plains occur concurrently with hail reports, SE

US tornadoes often occur without any hail. Again, this is likely a manifestation of the

convective mode of the tornadic storms, with supercells (which are strong hail

producers) dominating the tornadic storms in the Plains, and more linear modes (which

don't produce as much hail) being more likely in the SE US.
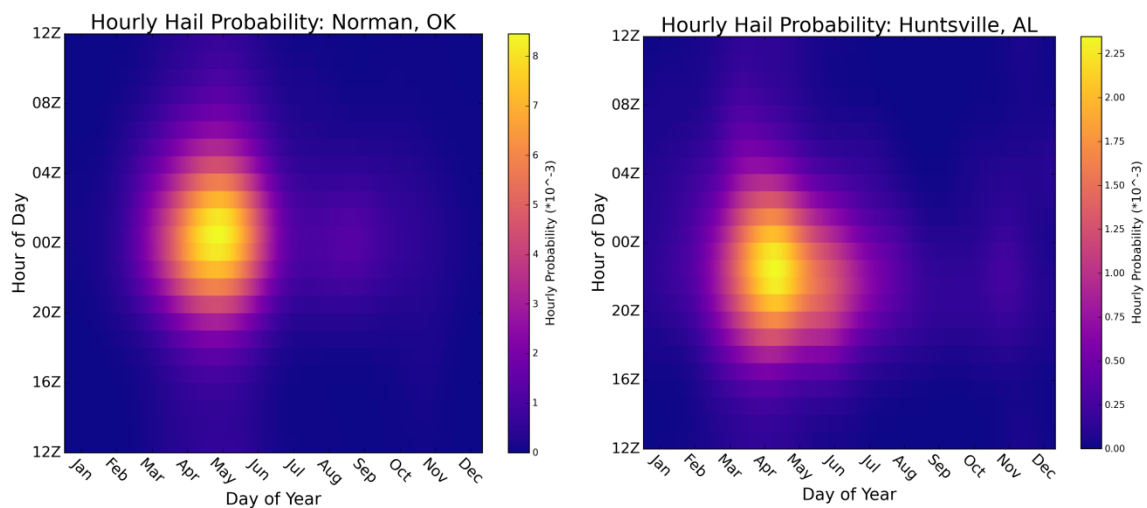
Figure 4.6: Heatmaps of hail probability for Norman, OK (left) and Huntsville, AL (right). Note the color bars are not the same.

Next, we plotted the location and relative magnitude of the peak hail probability

for 13 different days of the year (roughly once per month). This information is plotted

in figure 4.7. The size of the marker corresponds to the relative magnitude of the peak

(with the larger the marker indicating the larger threat), the color represents the time of

the year the peak occurred, and the location is plotted on the map. The peak hail

probabilities generally have a less variable peak location than the tornado peaks, which

spanned from the High Plains to the Washington, D.C. area. The hail peaks are

generally restricted to the Plains states, with the very early and very late year peaks

reaching into central Arkansas and northwest Louisiana. This difference again speaks to
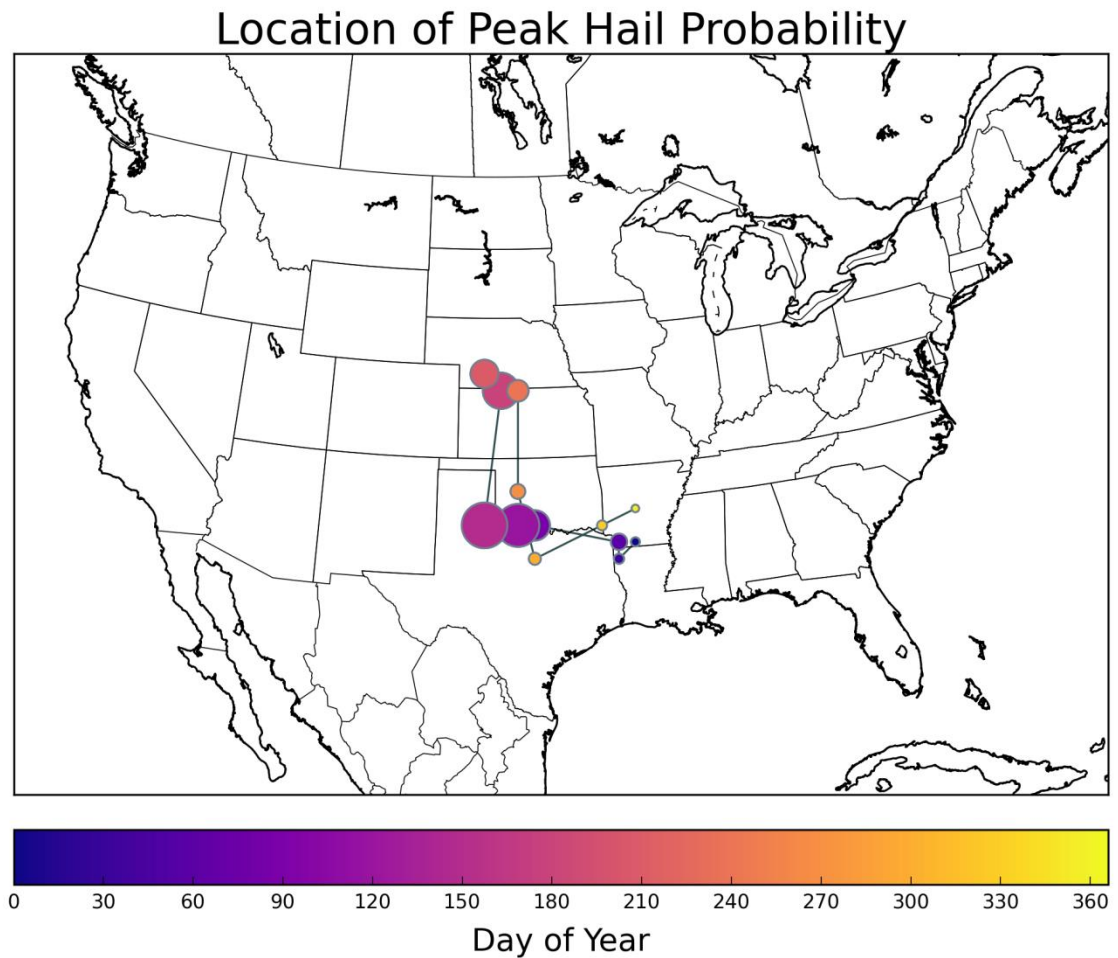
Figure 4.7: Location of peak hail probability once every 30 days. Color of the point corresponds to day of the year the peak occurred, and size of the point is proportional to the value of the maximum probability on that day.

the difference in threat type for the SE US versus the Plains. The SE US never

witnesses the peak in hail probabilities for the US, but they do witness the peak in

tornado probabilities for a large portion of the fall and winter months. This once again

57

indicates that tornadoes occurring in the SE US (particularly during the fall and winter months) are not usually accompanied by severe hail.

While the spatial breadth of the peaks was smaller than the tornado peaks, the difference in magnitude was much greater for the hail peaks. This can be seen by the change in the size of the peaks, which vary greatly from January to May. The very small peaks seen in the winter months indicate that very little hail occurs during this time, and what does occur is constrained to the southeastern Plains areas. There is then a sharp increase in peak probability (seen by the very large marker sizes in southwest Oklahoma and the southeast Texas panhandle) during the early spring months, and a westward movement in the peak location to the southern Plains. The peak then moves north into Kansas and Nebraska while maintaining most of the peak magnitude, before a steep decrease in magnitude and movement back into the Arkansas and Louisiana areas.

After seeing the peakedness of the annual cycle of hourly hail probabilities, we wanted to focus more on the daily cycle and how it differs from the daily tornado cycle. First, we plotted the maximum fraction of the total reports captured in a 4-hour period. However, this was a single 4-hour period for each point on the map, it didn't change by season or by synoptic setup. The fractions were calculated by adding up the four largest, consecutive hail probability values on each day, and then dividing that value by the sum of all 8784 hail probability values. This process was repeated for every point on the map, creating the pattern seen in Figure 4.8. One of the most interesting aspects of this plot is the low values that span the entire Mississippi river valley, from the Gulf to central Minnesota. Figure 3.15, which shows this same plot for the hourly tornado probabilities, shows the minimum fractions contained to the SE US, mainly along the

Gulf, with higher values further north. The difference in pattern could be attributed to the overall location of most severe hail reports. While the East Coast has higher fractions of reports captured in a 4-hour period, they also don't witness many reports, and never witness the peak in hail reports (as shown in Figure 4.7). The lower values in

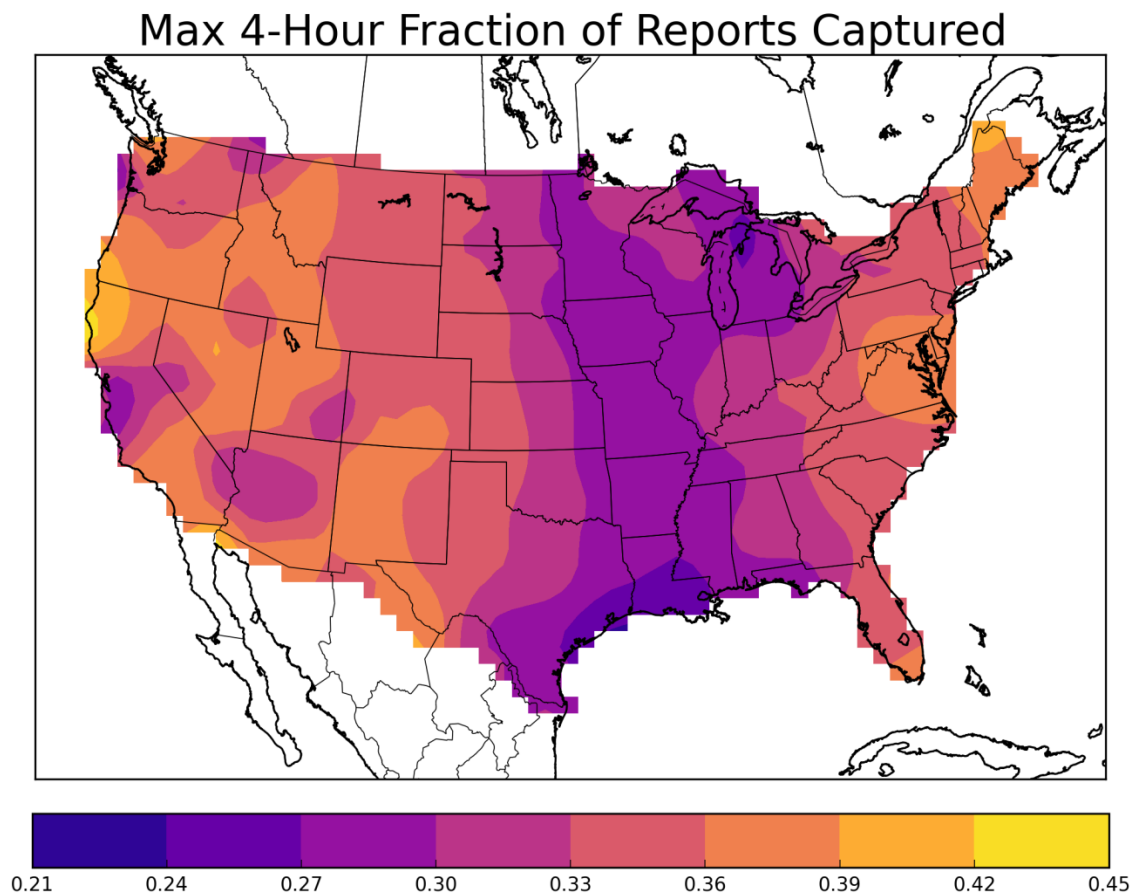Figure 4.8: The maximum fraction of the total number of daily hail events captured in a four-hour period.

the Mississippi river basin likely correspond to areas that see a fair amount of reports over a large fraction of the day and year. In other words, these areas experience hail during both the warm and cool season, and the diurnal cycle does not have a consistent impact on storm timing between the two seasons.

Regardless of how peaked the hourly hail probabilities are, we wanted to know when the 4-hour period calculated in Figure 4.8 started. This allows forecasters to understand when the majority of the hail threat for their area occurs. Figure 4.9 shows these values for each point in the US, with a truncated color bar from 18 UTC to 23 UTC. Similar to Figure 3.16, which shows the start time of the maximum 4-hour period for the hourly tornado probabilities, Figure 4.9 shows the start time becoming progressively earlier from the Plains to the East Coast. However, the start times for the hail probabilities show a much clearer pattern than the tornado start times. This is
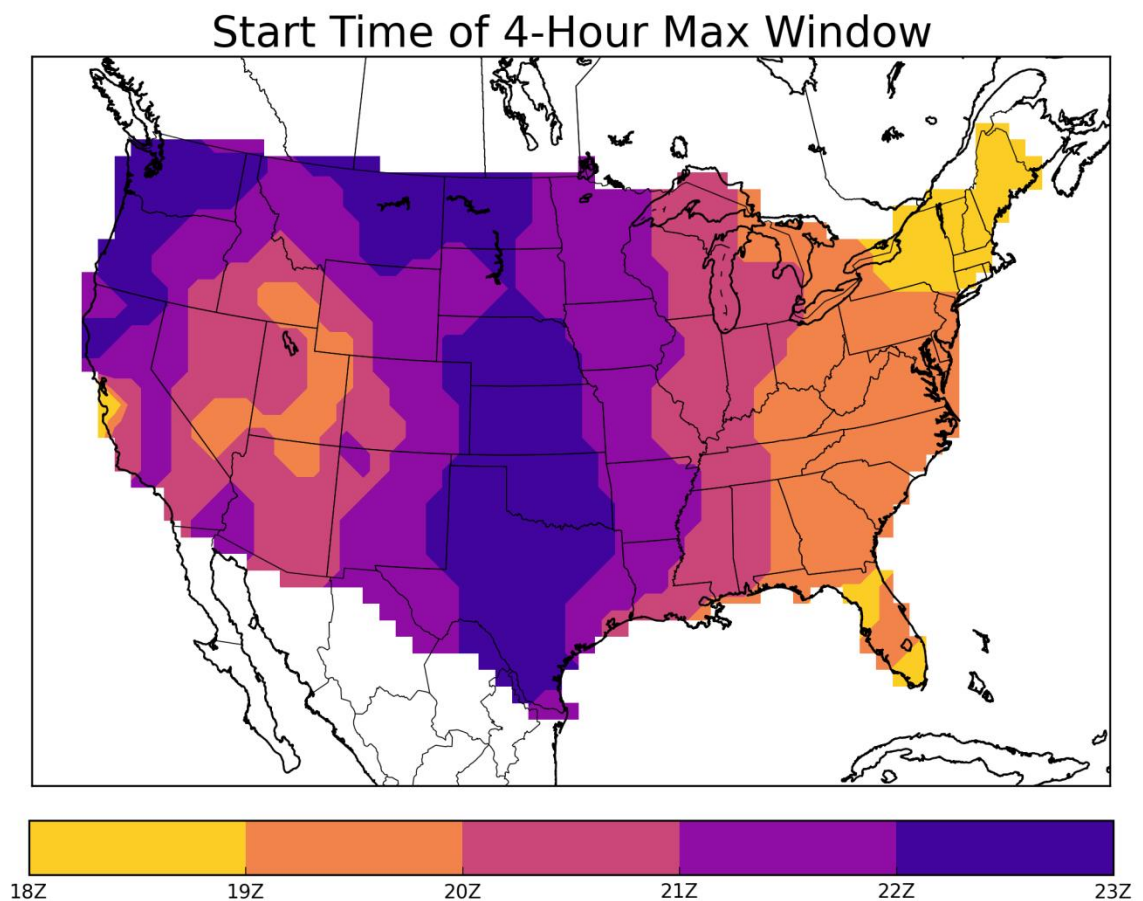
Figure 4.9: Start time of the four-hour period that captures the highest fraction of hail reports for every location across the country.

indicative of the idea that hail report times are very dependent on when the cap breaks and storms initiate. Tornado reports are much more dependent on other factors, including storm mode and evolution. The hail threat period can vary by more than four hours between the Plains states (which has a peak hail period from 22 UTC to 02 UTC) and New England (which has a peak hail period from 18 UTC to 22 UTC). This difference at first glance may not seem overly significant, but it is essentially the difference between having storms occur when most people are in cars versus when most people are at home or work. In New England, the time period corresponds to 2 pm to 6 pm local time for the maximum 4-hour period for hail reports. While there is a lot of

Figure 4.10: Fraction of total hours needed to capture 50% of the total annual hail threat.

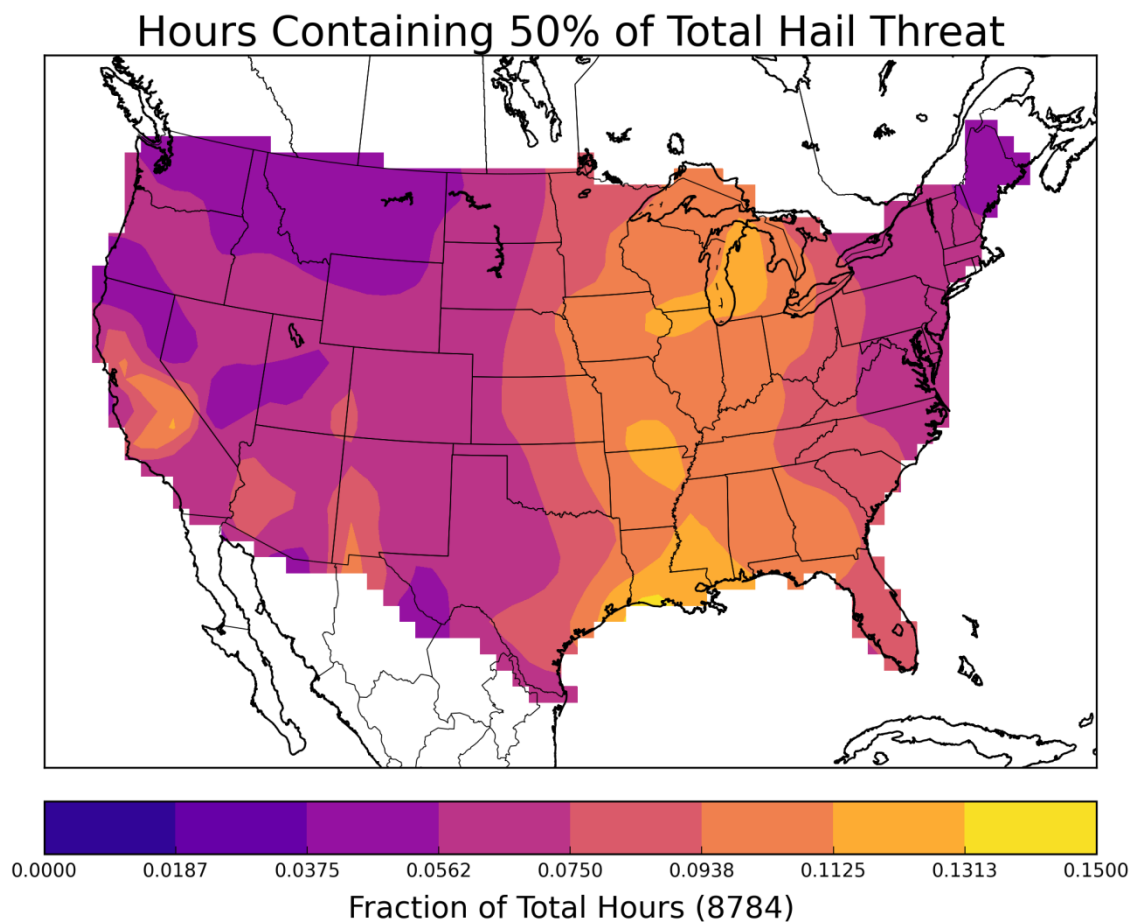travel in this time period, a much higher number of people travel between 4 pm and 9 pm, which is the maximum period in the Plains states. This time period corresponds perfectly to when most people are commuting from work or school. Obviously, it is much more ideal to have members of the community in a solid building than in a car when these storms hit. This creates a unique situation for forecasters in the central portion of the country, who need to tailor their forecasts to their users, who are much more likely to be travelling during peak severe weather times. These specific challenges need to be addressed in greater detail in the research community to better aid in the creation and dissemination of forecasts and decision support products.

Finally, we also looked at the minimum number of hours needed to contain at least 50% of the total hail threat. This fraction of the total 8784 hours is shown in Figure 4.10 for each point on the map. Similar to what was seen for the tornado threat, the lowest values are in the SE US areas. However, similar to Figure 4.8, those low values extend the entire length of the country, from the Gulf up into Minnesota and Wisconsin. Again, this is likely due to the overlap of areas that see a larger number of hail reports, but also see them during multiple seasons. The overall range of fractions is much smaller than what is seen for the tornado threat. Some areas need nearly 40% of the total hours to capture 50% of the total tornado threat, indicating that the annual and diurnal cycles are very variable. However, the "high" end of the fraction of hours needed to contain 50% of the hail threat is only 15% of the total hours. This indicates that hail is much more seasonally and diurnally driven as compared to tornadoes.

Chapter 5: Conclusions

An hourly climatology was developed for EF1 and greater tornadoes using 61 years of reports, and an hourly climatology of hail events greater than 1.25 inches was developed using 52 years of reports. All reports were gridded onto an 80 km lambert conic conformal grid by assigning all boxes with a report a 1, and all other boxes a 0. Grids were then smoothed spatially using a 120 km Gaussian kernel. Temporally, corresponding hours on each day were first smoothed with a 15 day kernel, and then adjacent hours were smoothed using a 2 hour kernel. This entire process was done to ensure that the annual cycle of events was represented without over smoothing the diurnal cycle. This resulted in adjacent daily sums of probabilities being nearly identical, and adjacent hourly probabilities differing with the diurnal cycle. The main goal of this work was to begin to understand the differences in the sub-daily distributions of hail events and tornadoes as compared to the annual distributions of such events.

Total annual tornado risks were found to peak in central Oklahoma and the Southern Plains as well as in the Mississippi and Alabama areas. However, while the total number of annual tornadoes was very similar, the distribution of those tornadoes was very different. The Plains have both a very peaked annual cycle as well as a very peaked diurnal cycle. This means that forecasters concerned with predicting tornadoes in these areas generally need to be concerned about 6 hours of the day for 3-4 months of the year. While this does not mean that forecasting these events is easy, it does mean that the climatological risk of these storms is very low outside of the peak time periods.

The southeastern portion of the US has a very different climatological risk of tornadoes. Neither the annual cycle nor the diurnal cycle is peaked; in fact it is nearly constant over all days and all times. This has implications for both forecasters and for emergency managers in these areas. Forecasters need to be aware that these storms can occur at any time of the day and nearly any time of the year. Therefore, community members also need to be prepared to take action at inconvenient times or locations (i.e. at school, work, or during the night, etc.).

The hourly hail climatology shows a similar pattern to the tornado climatology, with some minor differences. The total number of hail events in the southeast US is smaller than that in the Plains. Since these areas have a similar number of tornadoes per year, the lower number of hail events in the southeast indicates that there is a difference in the most common storm mode between the two regions. The Plains tends to experience storms that produce more hail (like supercells) and the Southeast tends to experience storms that don't produce large hail (like linear systems). Besides the lack of an annual or diurnal cycle, linear systems are capable of rapidly producing weak, erratic tornadoes, making forecasting an even bigger challenge.

Besides the difference in the total number of annual events, the hourly hail climatology is very similar to that of tornadoes. There is a more peaked annual and diurnal cycle in the Plains than in the Southeast, but the magnitude of the difference is much smaller than the differences in the tornado probabilities. Climatologically, hail events occur within a wider range of hours and days than tornadoes, which is consistent with previous climatological studies.

This hourly climatology begins the process of understanding the patterns and dependencies of these events on a sub-daily scale. The information allows researchers to understand how both the annual and the diurnal cycles vary in space and time, which has implications for how forecasters understand the background probabilities of these events and for how communities respond to hazardous weather occurrences. Forecasting these events on a sub-daily scale is going to require extensive knowledge on the distribution of these events on those scales. This work begins the process of analyzing these distributions and the implications they have for forecasting them. The results also summarize hourly tornado and hail frequencies, which have direct implications for mitigation procedures that need to be specific to the threat for each individual region of the United States.

Chapter 6: References

Allen, J. T., and M. K. Tippett, 2015: The characteristics of United States hail reports: 1955–2014. Electronic J. Severe Storms Meteor., 10 (3), 1–31.

Ashley, W. S., 2007: Spatial and temporal analysis of tornado fatalities in the United States: 1880–2005. Wea. Forecasting, 22, 1214–1228.

Anderson, C. J., C. K. Wikle, Q. Zhou, and J. A. Royle, 2007: Population influences on tornado reports in the United States. Wea. Forecasting, 22, 571–579, doi:10.1175/WAF997.1.

Brooks, H. E., and C. A. Doswell III, 2000: Climatological Risk of Strong and Violent Tornadoes in the United States. Second Symposium on Environmental Applications, Long Beach, CA, Amer. Meteor. Soc. [Available online at https://ams.confex.com/ams/annual2000/techprogram/paper_6471.htm.]

Brooks, H. E., and C. A. Doswell III, 2001b: Some aspects of the international climatology of tornadoes by damage classification, Atmos. Res.,56, 191–201, doi:10.1016/S0169-8095(00)00098-3.

Brooks, H. E., C. A. Doswell, and M. P. Kay, 2003a: climatological estimates of local daily tornado probability for the United States, Weather Forecasting, 18, 626–640, doi:10.1175/1520-0434(2003)018<0626:CEOLDT>2.0.CO;2.

Brooks, H. E., G. W. Carbin, and P. T. Marsh, 2014: Increased variability of tornado occurrence in the United States, Science, 346, 349–352, doi:10.1126/science.1257460.

Brooks, H. E., and D. J. Stensrud, 2000: Climatology of heavy rain events in the United States from hourly precipitation observations. Mon. Wea. Rev., 128, 1194–1201, doi:10.1175/1520-0493(2000)128,1194:COHREI.2.0.CO;2.

Carbin, G., P. Heinselman, and D. Stensrud, 2013: Current Challenges in Tornado Forecast and Warning. Int. J. on Mass Emerg. and Disasters, 31, 350-359. [Available online at http://www.ijmed.org/articles/632/download/.]

Chagnon, S. A., 1972: Examples of economic losses from hail in the U.S. J. Appl. Meteor., 11, 1128–1137.

Cintineo, J. L., T. M. Smith, and V. Lakshmanan, 2012: An objective high-resolution hail climatology of the contiguous United States. Wea. Forecasting, 27, 1235–1248, doi:10.1175/WAF-D-11-00151.1

Coleman, T. A., and P. G. Dixon, 2014: An objective analysis of tornado risk in the United States, Weather Forecasting, 29, 366–376, doi:10.1175/WAF-D-13-00057.1.

Concannon, P. R., H. E. Brooks, and C. A. Doswell III, 2000: Climatological risk of strong to violent tornadoes in the United States. Preprints, Second Symp. on Environmental Applications, Long Beach, CA, Amer. Meteor. Soc., 212–219.

Dixon, P. G., A. E. Mercer, K. Grala, and W. H. Cooke, 2014: objective identification of tornado seasons and ideal spatial smoothing radii, Earth Interact., 18, 1–15, doi:10.1175/2013EI000559.1.

Doswell, C. A., III, H. E. Brooks, and N. Dotzek, 2009: On the implementation of the enhanced Fujita scale in the USA, Atmos. Res., 93, 554-563, ISSN 0169-8095, doi:10.1016/j.atmosres.2008.11.003.

Doswell, C. A., III, and D. W. Burgess, 1988: On some issues of United States tornado
climatology. Mon. Wea. Rev., 116, 495–501.

Doswell, C. A., III, D. W. Burgess, and M. P. Kay, 2005: Climatological estimates of
daily local nontornadic severe thunderstorm probability for the United States.
Wea. Forecasting, 20, 577–595, doi:10.1175/WAF866.1.

Elsner, J. B., S. C. Elsner, and T. H. Jagger, 2014: The increasing efficiency of tornado
days in the United States, Clim. Dyn., doi:10.1007/s00382-014-2277-3.

Gall, M., K. A. Borden, and S. L. Cutter, 2009: When do losses count? Six fallacies of
natural hazards loss data, Bull. Amer. Meteor. Soc., doi:
10.1175/2008BAMS2721.1.

Hitchens, N. M., and H. E. Brooks, 2012: Preliminary investigation of the contribution
of supercell thunderstorms to the climatology of heavy and extreme precipitation
in the United States, Atm. Res. [Available online at
http://www.sciencedirect.com/science/article/pii/S0169809512002207.]

Kelly, D. L., J. T. Schaefer, R. P. McNulty, C. A. Doswell III, and R. F. Abbey, 1978:
An augmented tornado climatology. Mon. Wea. Rev., 106, 1172–1183.

Kis, A. K., and J. M. Straka, 2010: Nocturnal tornado climatology, Wea. Forecasting,
25, 545–561, doi:10.1175/2009WAF2222294.1.

Long, J. A., and P. C. Stoy, 2014: Peak tornado activity is occurring earlier in the heart
of "Tornado Alley", Geophys. Res. Lett., 41, 6259–6264,
doi:10.1002/2014GL061385.

NOAA National Weather Service Glossary [Available online at
http://forecast.weather.gov/glossary.php?word=CAP.]

Rasmussen, E. N., and D. O. Blanchard, 1998: A baseline climatology of sounding-
derived supercell and tornado forecast parameters, Weather Forecasting, 13,
1148–1164, doi:10.1175/1520-0434(1998)013<1148:ABCOSD>2.0.CO;2.

Rothfusz L., C. Karstens, and D. Hilderband, 2014: Next-Generation Severe Weather
Forecasting and Communication. EOS Transactions, 95. [Available online at
https://eos.org/project-updates/next-generation-severe-weather-forecasting-
communication.]

Schaefer, J. T., D. L. Kelly, and R. F. Abbey, 1986: A Minimum assumption tornado-
hazard probability model, J. Clim. Appl. Meteorol., 25, 1934–1945,
doi:10.1175/1520-0450(1986)025<1934:AMATHP>2.0.CO;2.

Schaefer, J. T., and R. Edwards, 1999: The SPC tornado/severe thunderstorm database,
in Preprints,11th Conf. on Applied Climatology, 6, 603–606, Am. Meteorol.
Soc., Dallas, Tex.

Schaefer, J. T., and R. S. Schneider, 2002: The robustness of tornado hazard estimates.
Preprints, Third Symp. on Environmental Applications, Orlando, FL, Amer.
Meteor. Soc., 4.2. [Available online at
https://ams.confex.com/ams/pdfpapers/27694.pdf.]

Silverman, B. W., 1986: Density Estimation for Statistics and Data Analysis. Monogr.
on Statistics and Applied Probability, No. 26, Chapman and Hall, 175 pp.

Smith, B. T., R. L. Thompson, J. S. Grams, C. Broyles, and H. E. Brooks, 2012:
Convective modes for significant severe thunderstorms in the contiguous United
States. Part I: Storm classification and climatology. Wea. Forecasting, 27, 1114–
1135.

NOAA Storm Prediction Center: Warning Coordination Meteorologist's Introduction.

[Available online at http://www.spc.noaa.gov/wcm/.]

Thom, H. C. S., 1963: Tornado probabilities, Mon. Weather Rev., 91, 730–736, doi:10.1175/1520- 0493(1963)091<0730:TP>2.3.CO;2.

Tippett, M. K., 2014: Changing volatility of U.S. annual tornado reports, Geophys. Res. Lett., 41, 6956–6961, doi:10.1002/2014GL061347.

Trapp, R. J., S. A. Tessendorf, E. S. Godfrey, and H. E. Brooks, 2005: Tornadoes from squall lines and bow echoes. Part I: Climatological distribution. Wea. Forecasting, 20, 23–34, doi:10.1175/WAF-835.1.

Verbout, S. M., H. Brooks, L. M. Leslie, and D. M. Schultz, 2006: Evolution of the U.S. tornado database: 1954–2003. Wea. Forecasting, 21, 86–93, doi:10.1175/WAF910.1.

Vescio, M. D., and R. L. Thompson, 2001: Subjective tornado probability forecasts in severe weather watches. Wea. Forecasting, 16, 192–195.